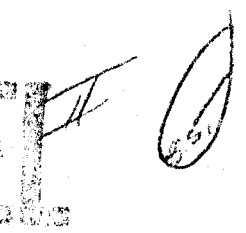


ARO 12931.1-EX

M.I.T. Fluid Dynamics Research
Laboratory Report No. 79-1

LEVEL 

PARAMETRIC STUDIES OF MODEL HELICOPTER BLADE SLAP AND ROTATIONAL NOISE

by

James E. Hubbard, Jr.,
N.G. Humbad,
Paul Bauer and
Wesley L. Harris

Department of Aeronautics and Astronautics
Fluid Dynamic Research Laboratory
Massachusetts Institute of Technology
Cambridge, Massachusetts 02139

DDC
RECEIVED
MAY 2 1979
ANT

February, 1979

DISTRIBUTION STATEMENT A
Approved for public release
Distribution Unlimited

ADA068181

ORIGINAL FILE COPY

M. I. T. Fluid Dynamics Research

Laboratory Report No. 79-1

THE VIEW, OPINIONS, AND THE FINDINGS CONTAINED IN THIS REPORT
ARE THOSE OF THE AUTHOR(S) AND SHOULD NOT BE CONSIDERED AS
AN OFFICIAL DEPARTMENT OF THE ARMY POSITION, POLICY, OR DE-
CISION, UNLESS SO DESIGNATED BY OTHER DOCUMENTATION.

PARAMETRIC STUDIES OF MODEL HELICOPTER BLADE
SLAP AND ROTATIONAL NOISE

by

James E. Hubbard, Jr.,

N. G. Humbad,

Paul Bauer

and

Wesley L. Harris

Department of Aeronautics and Astronautics
Fluid Dynamic Research Laboratory
Massachusetts Institute of Technology
Cambridge, Massachusetts 02139

February, 1979

79 04 27 055

SECURITY CLASSIFICATION OF THIS PAGE (When Data Entered)

REPORT DOCUMENTATION PAGE		READ INSTRUCTIONS BEFORE COMPLETING FORM
1. REPORT NUMBER M.I.T. Fluid Dynamics Research Laboratory Report No. 79-1	2. GOVT ACCESSION NO.	3. RECIPIENT'S CATALOG NUMBER 9
4. TITLE (and Subtitle) 6 Parametric Studies of Model Helicopter Blade Slap and Rotational Noise		5. TYPE OF REPORT & PERIOD COVERED Final Technical Report
7. AUTHOR(s) 10 James E. Hubbard, Jr., N. G. Humbad, Paul Bauer, and Wesley L. Harris		8. CONTRACT OR GRANT NUMBER(s) USARO DAAG29-76-C-0027 15
9. PERFORMING ORGANIZATION NAME AND ADDRESS Massachusetts Institute of Technology Dept. of Aeronautics & Astronautics Fluid Dynamics Research Laboratory Cambridge, MA 02139		10. PROGRAM ELEMENT, PROJECT, TASK AREA & WORK UNIT NUMBERS 12 79p.
11. CONTROLLING OFFICE NAME AND ADDRESS U.S. Army Research Office P.O. Box 12211 Research Triangle Park, NC 27709		12. REPORT DATE 12 February 1979
14. MONITORING AGENCY NAME & ADDRESS (if different from Controlling Office) Same as controlling office		13. NUMBER OF PAGES
16. DISTRIBUTION STATEMENT (of this Report) Distribution of this document is unlimited.		15. SECURITY CLASS. (of this report) Unclassified
17. DISTRIBUTION STATEMENT (of the abstract entered in Block 20, if different from Report) Distribution of this abstract is unlimited.		15a. DECLASSIFICATION/DOWNGRADING SCHEDULE
18. SUPPLEMENTARY NOTES Parts of this report were published in paper 79-0613 of the AIAA 5th Aeroacoustics Conference.		
19. KEY WORDS (Continue on reverse side if necessary and identify by block number) Helicopter, rotor acoustics, blade-slap, blade-vortex interaction noise, parametric studies, low tip speed, rotational noise, Mach number scaling of helicopter rotor noise.		
20. ABSTRACT (Continue on reverse side if necessary and identify by block number) A parametric study of model helicopter rotor blade slap due to blade/vortex interaction was studied in an anechoic wind tunnel. The parameters studied were blade number, advance ratio, pitch, and shaft angle. The separate effect of each parameter was studied with other parameters held fixed. The intensity of blade slap was found to decrease with an increase in the number of blades. As the advance ratio was increased to a maximum and then decreased with higher advance ratios indicating a blade slap envelope. The intensity (continued)		

DD FORM 1473 EDITION OF 1 NOV 65 IS OBSOLETE

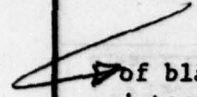
UNCLASSIFIED

SECURITY CLASSIFICATION OF THIS PAGE (When Data Entered)

140 250

JCB

Block 20.



of blade slap was observed to be directly proportional to pitch. The intensity increased with increasing pitch until unsteady lift was encountered, at which time the intensity rapidly diminished. As the rotor shaft angle was increased, the intensity of blade slap was found to decrease to a condition of no blade slap.

12

deg

Directivity measurements were made of blade slap due to blade/vortex interaction in the plane normal to the tunnel wind axis. No blade slap was encountered at the intersection of the rotor disc plane and the plane normal to the tunnel wind axis. The first indication of blade slap occurred at 30° below the rotor disc plane and increased in intensity, reaching a maximum intensity at 90° below the rotor. In all studies the presence of blade slap was determined subjectively by observing and listening to the transient acoustic signature.

An experimental investigation was also undertaken to verify the simplified Mach number scaling law for rotational noise from helicopter rotors proposed by Aravamudan, Lee, and Harris up to a tip Mach number of 0.39. Results include on axis and off axis comparisons between theory and experiment of the effect of tip Mach number. The overall trend of rotational harmonics was in good agreement with theoretical predictions using the scaling law. Experimental results also include the directivity of two- and three-bladed rotors.

TABLE OF CONTENTS

ABSTRACT 1

ACKNOWLEDGMENTS 3

LIST OF FIGURES 4

LIST OF TABLES 6

LIST OF SYMBOLS 7

I. MODEL HELICOPTER BLADE SLAP 9

 1.1 INTRODUCTION 9

 1.2 DATA REDUCTION PROCEDURES 12

 1.3 EXPERIMENTAL RESULTS AND DISCUSSION 14

II. MODEL HELICOPTER ROTOR ROTATIONAL NOISE 23

 2.1 INTRODUCTION 23

 2.2 MACH NUMBER SCALING LAW 24

 2.3 EXPERIMENTAL RESULTS AND DISCUSSIONS 25

III. CONCLUSIONS AND RECOMMENDATIONS 27

 3.1 CONCLUSIONS 27

 3.2 RECOMMENDATIONS 29

REFERENCES 31

TABLES 33

FIGURES 38

APPENDIX A 69

APPENDIX B 72

APPENDIX C 74

ACCESSION for		
NTIC	White Section	<input checked="" type="checkbox"/>
DOC	Soft Section	<input type="checkbox"/>
UNANNOUNCED		
JUSTIFICATION		
BY		
DISTRIBUTION/AVAILABILITY CODES		
Dist	AVAIL. and/or SPECIAL	
A		

ABSTRACT

A parametric study of model helicopter rotor blade slap due to blade/vortex interaction was studied in an anechoic wind tunnel. The parameters studied were blade number, advance ratio, pitch, and shaft angle. The separate effect of each parameter was studied with other parameters held fixed. The intensity of blade slap was found to decrease with an increase in the number of blades. As the advance ratio was increased in a blade slap "window," the intensity of the blade slap increased to a maximum and then decreased with higher advance ratios indicating a blade slap envelope. The intensity of blade slap was observed to be directly proportional to pitch. The intensity increased with increasing pitch until unsteady lift was encountered, at which time the intensity rapidly diminished. As the rotor shaft angle was increased, the intensity of blade slap was found to decrease to a condition of no blade slap.

Directivity measurements were made of blade slap due to blade/vortex interaction in the plane normal to the tunnel wind axis. No blade slap was encountered at the intersection of the rotor disc plane and the plane normal to the tunnel wind axis. The first indication of blade slap occurred at 30° below the rotor disc plane and increased in intensity, reaching a maximum intensity at 90° below the rotor. In all studies the presence of blade slap was determined subjectively by observing and listening to the transient acoustic signature.

An experimental investigation was also undertaken to verify the simplified Mach number scaling law for rotational noise from helicopter rotors proposed by Aravamudan, Lee, and Harris up to a tip Mach number of

0.39. Results include on axis and off axis comparisons between theory and experiment of the effect of tip Mach number. The overall trend of rotational harmonics was in good agreement with theoretical predictions using the scaling law. Experimental results also include the directivity of two- and three-bladed rotors.

ACKNOWLEDGMENTS

This research program was supported by the U. S. Army Research Office (contract No. DAAG 29-C-027).

LIST OF FIGURES

- Figure 1 Idealized Rotor Wake Geometry (Ref. 19)
- Figure 2 Vortex Paths in the Fore and Aft Plane (Ref. 1)
- Figure 3 Idealized Wave Shape of Blade Slap (Ref. 4)
- Figure 4 Blade Slap Boundary Mapping
- Figure 5 Blade Slap Boundary Mapping
- Figure 6 Blade Slap Boundary Mapping
- Figure 7 Schematic of Instrumentation Used in Data Acquisition
- Figure 8 Typical Pressure-Time History Trace of Blade Slap
- Figure 9 Typical Transient Recorder Trace of Blade Slap Profile
- Figure 10 Model Rotor Directivity Schematic
- Figure 11 Directivity Schematic Detail
- Figure 12 Pressure-Time History Study of Number of Blades Effect
- Figure 13 Roll-Up of the Wake Vortex Sheet and the Formation of the Tip Vortex (Ref. 15)
- Figure 14 Pressure-Time History Study of Blade Pitch Effect (5° Shaft Angle)
- Figure 15 Pressure-Time History Study of Blade Pitch Effect (0° Shaft Angle)
- Figure 16 Vortex Core Axis Parallel to Direction of Blade Motion
- Figure 17 Pressure-Time History Study of the Effect of Advance Ratio
- Figure 18 Single Rotor Blade/Vortex Interaction (Rigid Wake Assumption) (Ref. 15)
- Figure 19 Blade/Vortex Azimuthal Interaction Angles
- Figure 20 Coordinate System for Rotational Noise
- Figure 21 Schematic of Instrumentation for Acquisition of Acoustic Data
- Figure 22 Schematic of Instrumentation for Processing Rotational Noise

- Figure 23 Illustration of Effect of Periodic Sampling Techniques
- Figure 24 Mach Number Scaling for Rotational Harmonics of a Two-Bladed Rotor on Axis
- Figure 25 Mach Number Scaling for Rotational Harmonics of a Two-Bladed Rotor off Axis
- Figure 26 Mach Number Scaling for Rotational Harmonics of a Three-Bladed Rotor on Axis
- Figure 27 Mach Number Scaling for Rotational Harmonics of a Three-Bladed Rotor off Axis
- Figure 28 Directivity of Lower Harmonics of a Two-Bladed Rotor
- Figure 29 Directivity of Higher Harmonics of a Two-Bladed Rotor
- Figure 30 Directivity of Lower Harmonics of a Three-Bladed Rotor
- Figure 31 Directivity of Higher Harmonics of a Three-Bladed Rotor
- Figure C Noise Radiation Due to a Blade/Vortex Interaction (Ref. 16)

LIST OF TABLES

Table 1	Model Rotor Specifications
Table 2	Study of Blade Number Effect
Table 3	Study of Blade Pitch Effect
Table 4	Study of Advance Ratio Effect
Table 5	Blade Locations of Impulsive Signature
Table A	Correlation Factors

LIST OF SYMBOLS

B	Number of blades
C	Radial force component
C_m	Sound pressure amplitude of m^{th} sound harmonic
$C_{\lambda T}$	Complex Fourier coefficient of thrust
D	In-plane (drag) force component
G	Gross thrust of rotor
$J_n(Z)$	Bessel function of the 1^{st} kind, order n , argument Z
L_o	Total lift on one blade
M_e	Effective rotational Mach number
M_{or}	Component of hub convection Mach number in the direction of the observer
M_t	Rotor tip Mach number
N	Rotor speed in Hertz
$P(\bar{x}, n, M_t)$	Power spectral density of radiated sound at observer location \bar{x}
R	Rotor radius
SPL	Sound pressure level, decibels
T	Rotor thrust, lbs.
U_o	Hub convection velocity
U_t	Wind tunnel velocity, fps
V_t	Blade tip speed, fps
X_s	Spectrum function
Y	Distance of the observer from z axis
a_o	Speed of sound, fps
$a_{ot,od,oc}$	Steady Fourier components of thrust, in-plane, and radial force components

$a_{\lambda t, \lambda d, \lambda c}$	Fourier cosine components of thrust, in-plane, and radial forces
$b_{\lambda t, \lambda d, \lambda c}$	Fourier sine components of thrust, in-plane, and radial forces
c	Chord of rotor blade
i	Imaginary number $\sqrt{-1}$
m	Sound harmonic number
n	Loading harmonic number
r	Distance from hub to observer
r_1	Distance of the observer from the origin
x, y, z	Components of Cartesian coordinate system
τ	Source time
Γ	Vortex circulation strength
λ	Airloading harmonic number
Ω	Rotor speed, radians/second
α, β, ϕ	Angles - see Figure 20
ψ	Azimuth angle in rotor disc
ψ_0	360°
μ	Advance ratio

CHAPTER I

MODEL HELICOPTER BLADE SLAP

1.1 INTRODUCTION

Helicopter use and operation have become greatly limited due to radiated noise both mechanical and aerodynamic in nature. For example, reduction of community noise annoyance resulting from helicopter operation is clearly a requirement for civilian use. Similarly, in military use the signature of a helicopter has severely limited its military effectiveness. While the noise produced by the helicopter may emanate from one of many sources such as the powerplant, drive system, main rotor, etc., in the radiated far field, it is the aerodynamic noise which will dominate [1]. This noise may be divided into three categories as follows: 1) Rotational Noise, 2) High and Low Frequency Broadband Noise, 3) Blade Slap. Of these three mechanisms, blade slap when it occurs is the most prominent of the far field noise sources.

Classically there have been three main sources postulated for the generation of blade slap. These are: 1) Fluctuating forces due to blade/vortex interaction, 2) Fluctuating forces due to stalling and unstalling of the blade, 3) Local shock wave formation on portions of the blade. Evidence has been uncovered which suggests that the possibility of stall as a source of blade slap is very remote [1]. This research effort deals with the parametric study of model helicopter blade slap due to blade/vortex interaction. Several investigators have studied the production of blade slap due to blade/vortex interaction. Theoretical models by Widnall [2], and McCormick [3], have been presented in this regard.

In order to investigate this phenomenon one must be aware of the helicopter aerodynamics. The rotor blade tip exhibits a strong rotational vortex which affects the entire flow field of the rotor. There is a continuous shedding of vortices along the blade called a vortex sheet (Figure 1). The strongest of these vortices can be found at the blade tip. Each rotor blade then has its own vortex system which interacts with the system of some other blade to produce distortions of the rotor wake. The vortex sheet tends to roll up very rapidly into discrete vortex filaments behind the rotor. While there are many aerodynamic reasons causing the generation of these vortices, we will confine ourselves to the implication of said vortices on the far field radiated noise. Blade slap has been found to occur at those conditions where the vortex wake can be expected to pass very close to the rotor. For a single main rotor these conditions may occur during the autorotative descent, low power descents, steep turns, and decelerations.

A closer look at the aerodynamics involved in descent is useful in reaffirming the source of blade slap in this case. For descent rates of 70-150% of the induced hover velocity, a condition of large variations in thrust is experienced. This condition is formally known as the vortex ring state and is analogous to flying in one's own wake. The high rate of descent overcomes the normal downward induced flow on the inner blade sections. The flow is thus upward, relative to the rotor disc in these areas and downward elsewhere. This produces a secondary vortex ring in addition to the normal blade tip vortex system. This unsteady, turbulent flow over a large disc area gives rise to conditions which are highly conducive to blade/vortex interaction and hence the production of blade slap.

While it may be obvious how one can get blade/vortex interaction during descents, turns, etc., it may not be obvious as to whether or not blade/vortex interaction can occur during forward flight. It should be noted here that blade slap on full scale vehicles has been encountered during forward flight conditions. Smoke tests conducted by Simons, Pacifico and Jones [5] on a model rotor have shown that the path of the vortex core may indeed pass very close to the blades and in some cases this core path may actually pass through the rotor disc itself (Figure 2). This trend has been demonstrated in the theoretical studies of Crimi [6] and White [7]. It is this interaction caused by the vortex core passing through the rotor disc that is believed to cause blade slap during low speed forward flight. During high speed forward flight it is felt that blade slap is due to the formation of local shock waves on portions of the blade [8], [9].

Recent full scale experimental data obtained by Vause, Schmitz and Boxwell [10] have shown that three distinct types of impulsive noise can be radiated from a rotor (Figure 3). In these experiments a full scale UH-1H was flown between 80-150 knots and descent rates from 1-1000 feet per minute. The OV-1C "Mohawk" was used as a monitoring aircraft upon which a microphone was mounted and flown in front of the UH-1H at various angles below the tip path plane. The generalized noise signature is illustrated in Figure 3 and shows how each mechanism contributes to the total signature. It is also important to note here that, depending on the vehicle type and operating conditions, any one of these mechanisms may be dominant in the total makeup of the signature.

Section 1.2 discusses the techniques used to reduce the data and the advantages and disadvantages these techniques offer. A detailed discussion of the experimental results is given in Section 1.3. Finally, a summary of this research effort, with conclusions and recommendations for further work, is presented in Sections 3.1 and 3.2.

1.2 DATA REDUCTION PROCEDURE

Initially blade slap exploratory studies were carried out and "blade slap boundaries" were determined as a guide to planning more definitive studies. During this exploratory study the rotor advance ratio was varied at a given tunnel speed while holding the rotor shaft angle, blade pitch, and number of blades fixed. As the advance ratio was varied and blade slap encountered, boundary lines were plotted as a function of blade tip speed versus tunnel speed. Proceeding in this manner, blade slap boundaries were mapped for various blade numbers and shaft angle settings. These boundaries are presented in Figures 4-6. Having obtained these boundaries, tables of test parameters and conditions were constructed and used in a detailed parametric study of the model rotor blade slap noise.

The data gathered in this study were obtained in the form of peak to peak sound pressure levels of real-time transient noise signals, using the instrumentation shown in Figure 7. This form of the data was gathered by two different means. One procedure involved display of the signal on a dual trace oscilloscope. On one channel a one per revolution pulse was superimposed onto a one per blade pulse to

facilitate observation of shifts in the azimuthal location of the blade/vortex interaction. The one per revolution pulse was used as a triggering mechanism for the oscilloscope traces, while the one per blade signal could be used to observe shifts in the azimuthal location of the blade/vortex interaction. In addition, data reduced in this manner provides a means of monitoring the rotor rpm and may be used to determine the frequency of the slap signature itself. A typical oscilloscope trace of this type is presented in Figure 8. For very detailed studies of the signal the real-time pressure signal was stored via a transient recorder and output at a later time to an X-Y plotter, with time base (see Figure 9). Once these plots are obtained they may be calibrated using standard techniques. Data reduced in this manner proved excellent for making qualitative observations concerning the blade slap profile and vortex core movement.

Finally, directivity patterns of the blade slap noise were made. These patterns show the blade slap profile itself at various observer angles. This type of plot proved very useful in identifying the blade slap producing mechanism and its effect on the directivity of the sound. All directivity patterns were made in a plane normal to the tunnel wind axis at a radius of 52 inches from the rotor disc axis of rotation.

In all studies completed in this research effort, the presence of blade slap was determined subjectively by observing and listening to the transient acoustic signature. Several unsuccessful attempts were made to determine a quantitative definition and hence identification of blade slap. The results of these studies are presented in Appendix A.

1.3 EXPERIMENTAL RESULTS AND DISCUSSION

A study of one performance parameter with others fixed, on a rotor in flight, may be done in an anechoic wind tunnel. A parametric study of model helicopter rotor blade slap due to blade/vortex interaction was performed in the MIT anechoic wind tunnel facility. Specifically, the effects on the blade slap signal of the following parameters were investigated: number of blades, advance ratio, blade pitch and rotor shaft angle. Further details of aerodynamic and acoustic calibrations of this facility may be found in References [11] and [12]. The specifications of the rotor system used are given in Table 1. Further details of this system can be found in Reference [18].

The effects of blade number, advance ratio, blade pitch, and shaft angle on model helicopter rotor noise were studied. The tests were conducted using an inverted rotor. The radiated sound was measured via a microphone located 52 inches directly below the rotor disc plane. For the condition of these tests, this position was found to be the location of maximum intensity blade slap. In order to qualify the above statement a discussion of directivity is presented first. Referring once again to Figure 3, it is seen that the shape of the blade slap profile is primarily attributable to blade/vortex interaction, blade thickness effects due to high tip Mach number and effects due to radiated shock waves. The rotor tip speeds of the tests performed in this study were limited to approximately Mach 0.4 on an NACA 0012 airfoil with moderate twist. Under these conditions there are no transonic effects and hence any blade slap produced is purely the result of blade/vortex interaction. The probability of

stall being a blade slap producing mechanism was eliminated since a constant monitoring of the thrust gave no indication of the presence of severe stall. Once again the reader should be aware of the fact that the concept of stall as a blade slap producing mechanism is rapidly losing popularity as evidence is uncovered which suggests it to be a highly unlikely source of blade slap [1]. In the recent full scale tests performed by Schmitz and Boxwell [4], the directivity patterns of the UH-1 have been determined in forward flight. In these tests it can be seen that the intensity of the blade slap signature decreases as one moves from the rotor disc plane to a point directly beneath the helicopter. In fact, directly beneath the helicopter it would appear that there is no blade slap present at all and the most intense blade slap occurs roughly 13° below the rotor disc plane. It is important here to note that these tests were conducted at high tip transonic Mach numbers. Hence, as can be seen from their blade slap profiles, the dominant peak is that due to compressibility and thickness effects related to high tip speeds and high forward speeds. It is this dominant peak that is a maximum in the rotor plane and essentially vanishes beneath the helicopter. On the other hand, that portion of the total signal due to blade/vortex interaction appears to be absent in the rotor plane and increases in the direction moving beneath the helicopter. Once beneath the helicopter, however, this portion of the blade slap signature is of the same order or less as the rotational noise.

For the experiments of this study, where the blade slap produced is purely due to blade/vortex interaction, this same trend was observed.

Figures 10 and 11 are two representations of directivity patterns obtained under the conditions shown. All directivity patterns obtained in this study were made in a plane normal to the tunnel wind axis, at a radius of 52 inches from the rotor disc axis of rotation. No blade slap was encountered at the intersection of the rotor disc plane and the plane normal to the tunnel wind axis. The low frequency signals obtained are due mainly to turbulence noise caused by the positioning of the microphone in close proximity to the shear layer of the jet boundary in the open jet tunnel. At 20° below the rotor the first signs of blade slap become evident, but not dominant. Also at this angle the characteristic "beating" is audible. At 30° below the rotor plane blade slap has clearly developed and is dominant and continues to increase in intensity as one moves below the rotor disc. The directivity patterns for several other conditions were obtained and found to follow closely the trends observed here.

While the directivity patterns obtained in this study have been shown to agree with experimental data, there has also been theoretical work done which agrees with the trends observed here. As noted by Baush, Munch, and Schlegel [13] in their experimental study of blade slap, the air loading along the blade which gives rise to rotational noise is not very different from that which occurs during blade slap produced by blade/vortex interaction. The directionality associated with this form of blade slap therefore should not vary significantly from the non-slap case. The theoretical results of Ollerhead and Lawson [14], in which a model for the sound pressure amplitude of the m^{th} sound harmonic due to steady and fluctuating forces is developed (Appendix B), can then be used to plot the directionality. According to these results the detailed directionality is determined by

Bessel functions whose arguments are independent of the air loading harmonics and hence yield a directivity pattern very similar to the one obtained in this study.

It can be concluded then that the directivity pattern associated with the blade slap due to blade/vortex interaction is indeed very different from that due to high tip speed effects. While the former case yields maximum intensity directly beneath the helicopter, the latter has its maximum intensity located approximately 13° below the rotor plane. This result appears to be primarily due to the different types of air loading in each case.

In what follows the details of the parametric study are given. Before continuing, however, it should be noted that in the acquisition of sound pressure level-time history data during the experiments it was not possible to measure the sound pressure level of only the blade slap signal, i.e., the sound pressure levels consist of all the types of noise radiated from the model helicopter rotor. This is noted because it presents a problem when trying to interpret the data solely on the basis of relative SPL's.

The effect of number of blades on helicopter blade slap due to blade/vortex interaction was studied. Here a condition of blade slap was encountered for the two-bladed case, and then with other parameters unchanged the number of blades was increased to 3, then 4, respectively, and the effect on the signature observed. The conditions of this test are given in Table 2 and the results are plotted in Figure 12. Here it can be seen that as the number of blades is increased, the distinctive impulse signal vanishes. Also, the rotational noise components appear to increase in amplitude with increasing number of blades. This trend can readily be explained by observing first how the strength of the tip vortex itself is

affected and also the effect of increasing the number of blades on the tip path plane. From Leverton's theoretical study of blade slap [1], an idealized vortex core strength based on two dimensional potential flow is given by

$$\Gamma = \frac{2(G)}{V_t(B)R} \quad (1)$$

Figure 13 illustrates the formation of a tip vortex and identifies the circulation, Γ . While Eq. (1) is an idealization, it can be used to show trends effectively. For the case of the model rotor the gross weight can be taken to be of the same order of magnitude as the thrust being produced. Holding all of the above parameters fixed except the number of blades, it can be seen that as the number of blades is increased the vortex strength decreases proportionally. Hence, one would expect the intensity of the blade/vortex interaction to diminish. Furthermore, for the facility used in this work, the rotor did not have cyclic pitch control; therefore, as the number of blades increased, the tip path plane moved in a direction more in line with the free stream, hence less conducive to any blade/vortex interaction. It should be noted that under the normal conditions of the experiments presented in this study the tip path plane is tilted in a manner analogous to a helicopter in a descent mode. Under these conditions the segment of the tip vortex produced at the front of the rotor disc passes in very close proximity to the remainder of the disc, enhancing the likelihood of blade/vortex interaction. The same experiment with varying blade number was conducted in a different blade slap "window" and the trend was found to be identical to that described here.

Table 3 gives the conditions under which a study of the effect of pitch was determined. Figures 14 and 15 show the plotted results of that study. The profiles in the left of Figure 14 are for a two-bladed rotor with a shaft inclination of five degrees (5°), while those on the right are for a three-bladed rotor with the same shaft inclination. The profiles in Figure 15 are identical plots for zero degree (0°) shaft inclination. Basically, the trend suggests that as the pitch increases the rotor may go from a state where no blade slap is encountered to a state where blade slap is present and dominant. As the pitch increases further the intensity of the blade slap will increase and the impulsive nature of the profile becomes more and more evident. Finally, as the pitch is increased beyond a critical value, the blade slap diminishes and eventually disappears. There appears then to be a pitch envelope in which blade slap occurs. Once again insight into this trend may be achieved through use of Eq. (1). Replacing the gross weight by the rotor thrust and noting that as pitch increases, thrust increases in a manner directly proportional, one can see that the vortex strength increases with pitch. In addition the tip path plane takes on a steeper angle with respect to the free stream and the coning angle increases, placing the rotor in a descent mode. The latter occurrences produce ideal conditions for blade/vortex interaction while an increase in vortex circulation strength ensures that when this interaction takes place the resulting blade slap will be increasing in intensity as pitch is increased. Finally, as the pitch reaches a critical value, the blade slap decreases and eventually disappears. This critical value is believed to be the onset of stall as evidenced visually by a highly unstable tip path

plane and thrust. In the cases presented in this work this stall occurs first at the blade root and progresses toward the tip due to the geometry of the blades used. The pitch angles given are those corresponding to blade pitch at the tip of the blades. The actual pitch at the root is 8° higher due to an 8° negative twist from root to tip.

While performing this study an interesting effect was observed which warrants discussion. A closer look at the first profile in the left column of Figure 15 shows a reversal in the sign of the pressure gradient from one blade to the other which is not evident in the other profiles. This effect was observed to occur in a random manner during the acquisition of data. It is believed to be primarily due to the interaction geometry present at a given instant. Figure 16 illustrates an interaction path which a blade may take with respect to the vortex core. A blade intersecting the vortex near point A would experience first a negative velocity gradient followed a short time later by a positive velocity gradient, resulting in a rapid change in blade angle of attack and impulsive blade loading. Conversely, blade interactions near point C would result in an initial positive velocity gradient followed by a negative gradient again resulting in an impulsive loading of the blade. The strength of the interaction and subsequent blade slap intensity is governed by the angle of the interaction with the core and the distance of the interaction from the vortex core center line. It can be seen then that the interaction geometry clearly affects orientation of the blade slap profile as well as the intensity.

Figures 14 and 15 may also be used to observe the effect of increasing shaft angle. It should be noted that a blade slap boundary could not be

determined for tested conditions for shaft angles of ten degrees (10°) and above.

At these shaft angles the tip path plane is not oriented to enhance blade/wake interaction. The tip path plane in this configuration is in a low speed forward flight condition or ascent mode. Neither of these modes is likely to produce strong blade/vortex interaction. From these plots it is evident that as the rotor shaft angle is increased and other parameters are held constant, consistent with remaining in the blade slap window, it can be seen that the intensity of the blade slap decreases and eventually vanishes. As shaft angle increases the tip path plane moves in a manner equivalent to a transition from descent to forward flight and possibly ascent.

Finally, the effect of advance ratio was studied under the conditions given by Table 4. Here a varying advance ratio is achieved by varying the tunnel speed. In these tests, the following parameters were maintained constant: number of blades, shaft angle, pitch, and rotor rpm. The results of this study are illustrated in Figure 17. These plots show that as advance ratio is increased from a condition of no blade slap, blade slap is encountered, grows in intensity and then vanishes with a further increase in advance ratio. Once again there is an advance ratio envelope in which blade slap is produced. It should be noted that this envelope correlates remarkably well with the blade slap boundaries determined during the exploratory phase of this study shown in Figures 4-6. In order to understand this trend, one may look at how the advance ratio influences the geometry of the blade/vortex interaction. A first suspicion might be that the vortex strength is increasing with advance ratio. If we note

that

$$\mu = \frac{U_t}{V_t} \quad (2)$$

and use this in conjunction with Eq. (1) to get

$$\Gamma = \frac{2\mu(G)}{U_t BR} \quad (3)$$

We find that since advance ratio is being varied by increasing the tunnel speed, the vortex core strength remains approximately constant. Figure 18 is a schematic of a single rotor during blade/vortex interaction. The interaction angle has a significant effect on the sound pressure level as reported by Pegg [16] and proven theoretically in the work of Wright [17]. (Appendix C) The greater the angle of azimuthal intersection, the more intense will be the radiated noise. A low azimuthal angle would correspond to the rotor being almost aligned with the free stream during the interaction. Table 5 in conjunction with Figure 19 shows the azimuthal locations of the blade during increasing advance ratio for the rotor and facilities used in this study under the conditions given [18]. As the advance ratio is increased the azimuthal position of the interaction shifts, and does so in the direction of shallow azimuthal angles of interaction. This results in a gradual decrease in the intensity of blade slap with an increase in advance ratio as indicated by the works mentioned previously [16, 17].

CHAPTER II

MODEL HELICOPTER ROTOR ROTATIONAL NOISE

2.1 INTRODUCTION

Helicopter rotors generate complex acoustic signatures. A variety of mechanisms have been postulated and studied both theoretically and experimentally to assess their possible significance as noise sources. The low frequency sound radiated by a lifting rotor at low to moderate tip speeds is essentially due to the time varying pressure distribution on the blade. The low frequency spectrum of such pressure fluctuations contains discrete narrow peaks which occur at an integer multiple of blade passage frequency. This is often termed as "rotational noise." Typical spectrum of rotational noise may extend over a frequency range of approximately thirty times the blade passage frequency.

The rotational noise spectra of typical helicopter rotors are strongly dependent on the blade tip Mach number, in addition to other helicopter performance parameters. Most model rotor systems cannot simulate the high tip Mach numbers of real helicopters. Therefore, Aravamudan, Lee, and Harris [20] derived a simple Mach number scaling law and experimentally verified it up to rotational Mach number of about 0.20. In this section we have presented experimental results at higher tip Mach numbers to verify the scaling law. In Section 2.2 we briefly review details of the scaling law. The experimental verification of the scaling procedure is discussed in Section 2.3.

2.2 MACH NUMBER SCALING LAW

The contents of this section are derived from References [20-22]. It seems that the rotational noise of subsonic rotors is mainly attributed to force and thickness terms. The relative importance of force, force derivative and thickness terms depends on the rotor blade Mach number. At low tip Mach numbers the product of source strength and acoustic efficiency is greater for force derivative terms than that for force and thickness terms. It is shown in References [20, 21] that if the effective Mach number, $M_e = M_t \sin \alpha / (1 - M_{or})$ (where M_t is rotational tip Mach number, and M_{or} is the component of the hub convection Mach number in the direction of the observer) is less than 0.65, then thickness and force terms are relatively unimportant in comparison with the force derivative term. Incorporating this dominant balance argument, Reference [20] contains a derivation of a Mach number scaling law using the expressions for the far field acoustic radiation due to a rotating fluctuating point force. The final form of the Mach number scaling law is given as

$$P(\bar{x}_2, n_1, M_{t_2}) = P(\bar{x}_1, n, M_{t_1}) \left(\frac{M_{t_2}}{M_{t_1}} \right)^6 \left(\frac{c_2}{c_1} \right)^2 \left(\frac{r_2}{r_1} \right)^2 \left(\frac{\cos \alpha_2}{\cos \alpha_1} \right)^2 \left[\frac{1 - \mu_1 M_{t_1} (\cos \alpha_1 \cos \beta_1 + \sin \alpha_1 \sin \beta_1 \cos \phi_1)}{1 - \mu_2 M_{t_2} (\cos \alpha_2 \cos \beta_2 + \sin \alpha_2 \sin \beta_2 \cos \phi_2)} \right]^2 \quad (4)$$

and is valid only when $[C_{\lambda T}]_1 = [C_{\lambda T}]_2$ and $[M_t Y / r_1]_1 = [M_t Y / r_1]_2$. In the above, subscripts 1 and 2 denote quantities from two different sets being compared. In the case of wind tunnel test setup where rotor and microphone positions are fixed, $M_{or} = 0$, and if the measurements are made

in a plane perpendicular to the flow direction, the Mach number scaling formula takes the simple form

$$P(\bar{x}_2, n, M_{t_2}) = P(\bar{x}_1, n, M_{t_1}) \left(\frac{M_{t_2}}{M_{t_1}} \right)^6 \left(\frac{c_2}{c_1} \right)^2 \left(\frac{r_1}{r_2} \right)^2 \left(\frac{\cos \alpha_2}{\cos \alpha_1} \right)^2 \quad (5)$$

It may again be summarized here that the above scaling law is valid for effective Mach number, M_e less than 0.65 and for geometrically similar blades. Scaling also requires the two relationships: $[C_{\lambda T}]_1 = [C_{\lambda T}]_2$ and $(M_t Y/r_1)_1 = (M_t Y/r_1)_2$.

2.3 EXPERIMENTAL RESULTS AND DISCUSSION

The experimental investigation was basically a continuation of work done by Aravamudan, Lee, Harris [20] and by Aravamudan and Harris [21] for higher rotational Hp Mach numbers. Details of experimental setup, instrumentation, and measurements, and data analysis are not repeated here. The maximum rotational tip Mach number with the present experimental setup was 0.391 in comparison with 0.20 of References [20] and [21]. Since the effective Mach number is less than 0.65, the Mach number scaling relationships given by Eqns. (1) and (2) are still valid and are used to verify the experimental results.

Figures 21 and 22 depict the schematic of instrumentation for acquisition of acoustic data and for processing rotational noise respectively. A periodic sampling technique was used in determining the intensity of rotational harmonics. Figure 23 illustrates the effect of periodic sampling technique. Waveform and corresponding low-frequency narrow band spectra of raw and processed signal are compared.

Figures 24 and 25 depict the results of the Mach number scaling formula for rotational harmonics of a two-bladed rotor for on axis and off axis measurements, respectively. Also shown in Figures 26 and 27 is the comparison between theory using the Mach number scaling of Reference [20] and experimental data for rotational harmonics of a three-bladed rotor, on axis and off axis measurements, respectively. In the case of on axis comparisons, the experimental results at a tip Mach number of 0.244 were used to predict the sound pressure levels at other Mach numbers. For the off axis comparison, the experimental results at a tip Mach number of 0.244 and $\alpha = 42.5^\circ$ were used to predict the sound pressure levels at other Mach numbers. It is seen from Figures 24-27 that the overall trend of rotational harmonics is in good agreement with theoretical predictions using the scaling law.

Figures 28 and 29 show the directivity of lower and higher rotational harmonics respectively of a two-bladed rotor. Figures 30 and 31 depict the directivity of rotational harmonics of a three-bladed rotor. The directivity data were obtained by positioning the microphones at 10° intervals and using the periodic sampling technique. As can be seen from these figures, the directivity pattern is dependent on the harmonic number.

CHAPTER III

CONCLUSIONS AND RECOMMENDATIONS

3.1 CONCLUSIONS

A parametric study of model helicopter blade slap due to blade/vortex interaction has been performed in the MIT 5x7¹/₂ foot anechoic wind tunnel. The parameters studied were blade pitch, blade number, advance ratio and shaft angle. The separate effects of each parameter were studied with the other parameters fixed consistent with operation in a blade slap "window." In all cases, the tip path plane was allowed to vary due to the constraint mentioned above and the absence of cyclic control in our model. In addition to the above parametric study a detailed study of the directivity associated with such blade slap was completed.

The intensity of the blade slap signature was found to vary inversely with the number of blades. This is primarily due to a decrease in the span loading and vortex circulation strength as the number of blades increases. In the model rotor used, a decrease in span loading also caused the tip path plane to move in a direction less conducive to blade/vortex interaction.

The intensity of the blade slap was found to be directly proportional to the blade pitch. This is due once again to an increase in disc loading as well as tip vortex strength with an increase in pitch. Furthermore, an increase in pitch caused the rotor disc to tilt in a manner which corresponds to a descent mode, a condition ideally suited for blade/vortex interaction. The increase in intensity with a corresponding increase in

pitch was found to occur until rapid fluctuations in lift, as evidenced by a highly unstable tip path plane, caused a decrease and eventual vanishing of blade slap.

As the advance ratio is varied the azimuthal angle of blade/vortex interaction shifts. For very low advance ratios the azimuthal interaction angle is very shallow and hence the interaction is not a strong one. As the advance ratio is increased the angle of interaction increases until a very strong blade/vortex interaction occurs, resulting in the production of intense blade slap. As further increases in advance ratio are made, a gradual reduction and eventual disappearance of the impulsive noise occurs. This is again due to a gradual decrease in the interaction angle. A similar result of sound pressure level on the azimuthal location of the interaction has been shown by Wright [17] and Pegg [16].

The intensity of blade slap was found to vary inversely with shaft angle for a rotor without cyclic pitch. This trend is primarily due to the orientation of the tip path plane in the free stream. As the shaft angle is increased the tip path plane shifts from a position corresponding to a descent mode to one of a forward flight or ascent mode which is less conducive to blade/vortex interaction.

A study of directivity revealed the most intense blade slap directly beneath the rotor and not 13° below as observed in other works concerned with high speed flight. This is due to the difference in the source responsible for the blade slap in each case. In this work the blade slap produced is due to only blade/vortex interaction with no transonic effects present and hence yields a directivity very similar to that of the non-blade

slap case. When transonic effects are present, as in the case of previous work [10], the directivity will be dramatically altered primarily due to the difference in the air loading of blades in each case.

The experimental investigation has been undertaken to verify the simplified Mach number scaling law for rotational noise from helicopter rotors by Aravamudan, Lee and Harris. This investigation covers tip Mach number range of about 0.20 to 0.40. On axis and off axis comparisons between experiment and theory are presented for two- and three-bladed rotors. Experimental results are found to be in good agreement with theoretical predictions using the scaling law. It is seen from experimental results of the directivity of two- and three-bladed rotors that the directivity pattern is dependent on the harmonic number.

3.2 RECOMMENDATIONS

While the results of this study have been very revealing as to the parameters involved in blade slap due to blade/vortex interaction, many questions have arisen. It is felt by the authors that the controversy of intermittent stall as a possible source of blade slap must be resolved. Definitive studies in this area are clearly warranted and well within the capability of present day researchers. It is recommended then that a detailed study of the effects of intermittent stall on helicopter blade slap be made for both subsonic and transonic tip speeds. In addition it is recommended that a study of the effects of turbulence on the intensity of blade slap due to blade/vortex interaction be undertaken as the next logical step in understanding the mechanisms of blade slap produced by full scale helicopters. The effects of said turbulence on the movement

of the vortex core and blade/vortex interaction angle should be studied with the aid of modern visual techniques such as smoke indicators used in conjunction with strobe photography. The latter study would clearly give greater insight into the advance ratio effect on blade slap and the highly complex interaction geometry involved.

This reported investigation of helicopter rotor rotational noise should be extended further at higher tip Mach numbers to verify the validity of the scaling law up to an effective Mach number of about 0.65.

REFERENCES

1. Leverton, J.W., "Helicopter Noise-Blade Slap; Part 1: Review and Theoretical Study," NASA CR-1221, October 1968.
2. Widnall, S., Chu, S., and Lee, A., "Theoretical and Experimental Studies of Helicopter Noise Due to Blade-Vortex Interaction," Helicopter Noise Symposium, Durham, North Carolina, September 1971.
3. McCormick, B.W., "Studies Relating to Steady and Unsteady Aerodynamics of Helicopter Noise Symposium," Durham, North Carolina, September 1971.
4. Schmitz, F.H., and Boxwell, D.A., "In-Flight Far Field Measurement of Helicopter Impulsive Noise," Journal of the American Helicopter Society, Vol. 21, No. 4, October 1976.
5. Simons, I.A., Pacifico, R.E., and Jones, J.P., "The Movement, Structure and Breakdown of Trailing Vortices from a Rotor Blade," CAL/USAAVLABS Symposium Proceedings, Vol. 1, 1966.
6. Crimi, P., "Prediction of Rotor Wake Flows," CAL/USAAVLABS Symposium Proceedings, Vol. 1, Propeller and Rotor Aerodynamics, June 1966.
7. White, A.P., "VTOL Periodic Aerodynamic Loadings: The Problems, What is Being Done and What Needs to be Done," Journal of Sound and Vibration, Vol. 4, No. 3, pp 282-304, 1966.
8. Cox, C.R., and Lynn, R.R., "A Study of the Origin and Means of Reducing Helicopter Noise," Bell Helicopter Co., USATCREC Technical Report 62-73, U.S. Army Transportation Research Committee, Ft. Eustis, VA., November 1962.
9. Tangler, J.L., "Schlieren and Noise Studies of Rotors in Forward Flight," presented at the 33rd Annual National Forum of the American Helicopter Society, May 1977.
10. Vause, C.R., Schmitz, F.H., and Boxwell, D.A., "High-Speed Helicopter Impulsive Noise," Preprint 1004, 32nd Annual National Forum of the American Helicopter Society, May 1976.
11. Widnall, S.E., Harris, W.L., Lee, A., and Drees, H.M., "The Development of Experimental Techniques for the Study of Helicopter Rotor Noise," NASA CR-137684, 1974.
12. Harris, W.L., and Lee, A., "The Development of Experimental Techniques for the Study of Helicopter Rotor Noise," AIAA 2nd Aeroacoustics Conference, March 1975.
13. Bausch, W.E., Munch, C.L., and Schlegel, R.G., "An Experimental Study of Helicopter Rotor Impulsive Noise," USAAVLABS Technical Report 70-72, June 1971.

14. Lawson, M.V., and Ollerhead, J.B., "A Theoretical Study of Helicopter Rotor Noise," Journal of Sound and Vibration, Vol. 9, No. 2, pp 197-222, 1969.

15. Chu, Sing, "An Unsteady Lifting Surface Theory for the Wing-Gust Interaction and Its Application," Ph.D. Thesis, MIT, 1974.

16. Pegg, R.J., and White, R.P., "Some Measured and Calculated Effects of Tip Vortex Modification on Subsonic Impulsive Noise," AIAA 4th Aeroacoustics Conference, October 1977.

17. Wright, S.E., "Discrete Radiation from Rotating Periodic Sources," Journal of Sound and Vibration, Vol. 17, No. 4, pp 437-498, 1971.

18. Lee, A.Y., "An Experimental and Theoretical Study of Helicopter Rotor Noise," Ph.D. Thesis, MIT, 1975.

19. Gessow, A., and Myers, G.C., "Aerodynamics of the Helicopter," F. Ungar Pub. Co., New York, 1967.

20. Aravamudan, K.S., Lee, A. and Harris, W.L., "A Simplified Mach Number Scaling Law for Helicopter Rotor Noise," Journal of Sound and Vibration (1978), 57 (4), pp 555-570.

21. Aravamudan, K.S., Harris, W.L., "Experimental and Theoretical Studies on Model Helicopter Rotor Noise," MIT Fluid Dynamics Research Lab. Report No. 78-1, Jan. 1978.

22. Humbad, N.G., "Correction to a paper entitled, A Simplified Mach Number Scaling Law for Helicopter Rotor Noise," to appear in J. of Sound and Vibration.

TABLE 1
MODEL ROTOR SPECIFICATIONS

Radius (b)	25 inches (64.1 cm)
Chord (c)	2 inches (5.13 cm)
Number of blades (B)	1 to 8
Section	NACA 0012
Twist	- 8°
Shaft tilt capability	± 20°
Maximum RPM	2700
Testing RPM	Variable, from 400 RPM to 1100 RPM
Lead-lag	None
Cycle pitch	None
Collective pitch	By adjusting pitch of individual blade

TABLE 2
STUDY OF BLADE NUMBER EFFECT

<u>Number of Blades</u>	<u>Tunnel Speed (fps)</u>	<u>Blade Pitch</u>	<u>Shaft Angle</u>	<u>Rotational Speed (rpm)</u>
2	51.3	5°	0°	1300
3	51.3	5°	0°	1300
4	51.3	5°	0°	1300

TABLE 3

STUDY OF BLADE PITCH EFFECT

<u>Number of Blades</u>	<u>Tunnel Speed (fps)</u>	<u>Blade Pitch</u>	<u>Shaft Angle</u>	<u>μ (Advance Ratio)</u>
2	44	3°	5°	.26
2	44	8°	5°	.26
2	44	10°	5°	.26
2	44	13°	5°	.26
3	44	3°	5°	.28
3	44	8°	5°	.28
3	44	10°	5°	.28
3	44	13°	5°	.28
2	44	3°	0°	.17
2	44	5°	0°	.17
2	44	8°	0°	.17
2	44	10°	0°	.17
2	44	13°	0°	.17
3	44	3°	0°	.22
3	44	5°	0°	.22
3	44	8°	0°	.22
3	44	10°	0°	.22
3	44	13°	0°	.22

TABLE 4

ADVANCE RATIO EFFECT

<u>Number of Blades</u>	<u>Tunnel Speed (fps)</u>	<u>Blade Pitch</u>	<u>Shaft Angle</u>	<u>Advance Ratio</u>
2	29.3	5°	0°	.18
2	36.7	5°	0°	.22
3	20.5	5°	0°	.16
3	29.3	5°	0°	.22
3	36.7	5°	0°	.28

TABLE 5

BLADE LOCATION OF IMPULSIVE SIGNATURE

<u>B</u>	<u>Rotational Speed rpm</u>	<u>Tunnel Speed mph</u>	<u>Pitch Angle</u>	<u>Shaft Angle</u>	<u>Azimuth Angle</u>
2	1100	30	5°	0°	50-230°
2	1100	40	5°	0°	80-260°
2	1100	50	5°	0°	10-190°

Fig. 1 IDEALIZED ROTOR GEOMETRY

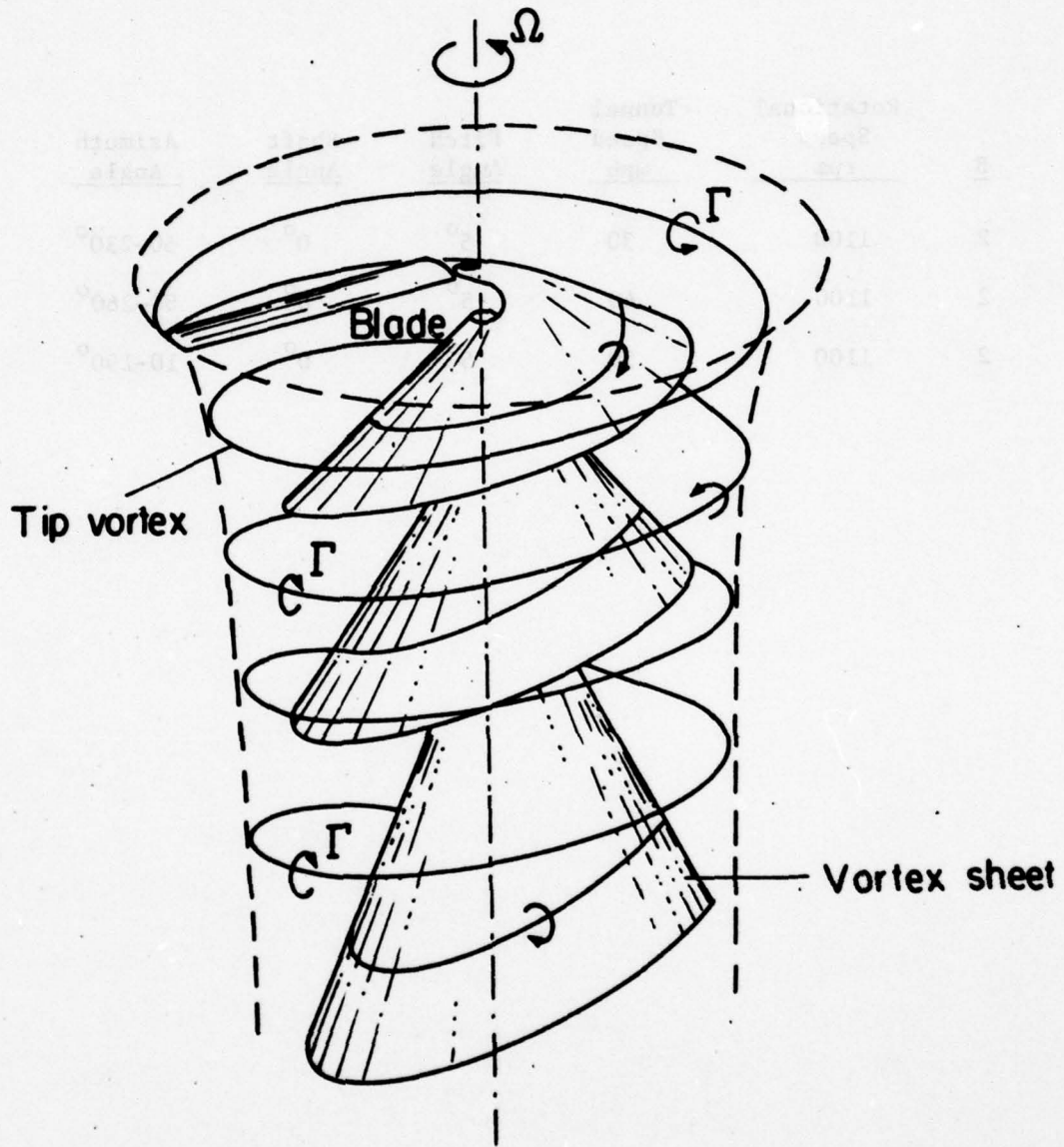


FIG. 1 IDEALIZED ROTOR GEOMETRY

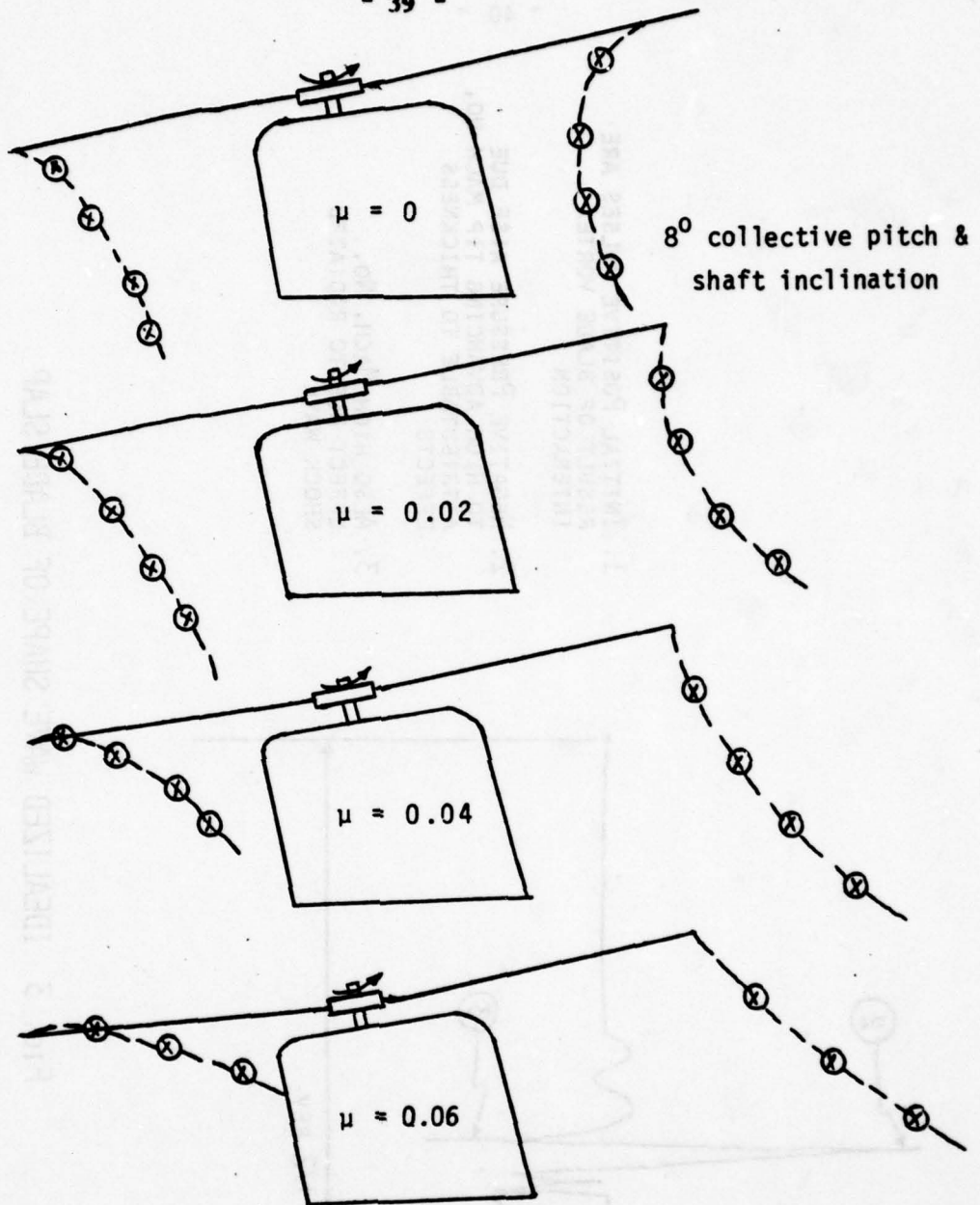


FIG. 2 VORTEX PATHS IN THE FORE-AND-AFT PLANE

1. INITIAL POSITIVE PULSES ARE RESULT OF BLADE VORTEX INTERACTION
2. NEGATIVE PRESSURE RISE DUE TO HIGH ADVANCING TIP MACH NO. ATTRIBUTABLE TO THICKNESS EFFECTS
3. ALSO HIGH MACH. NO. EFFECT DUE TO RADIATED SHOCK WAVE

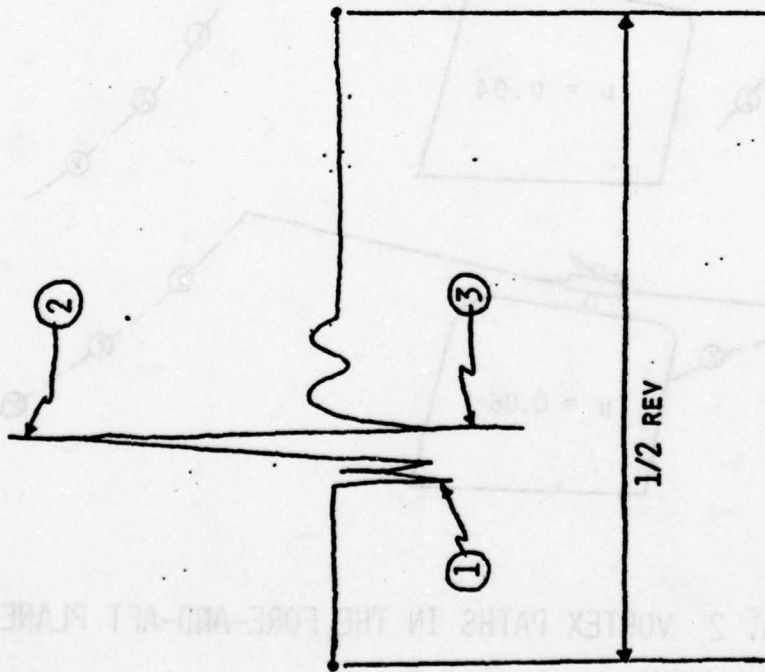


FIG. 3 IDEALIZED WAVE SHAPE OF BLADE SLAP

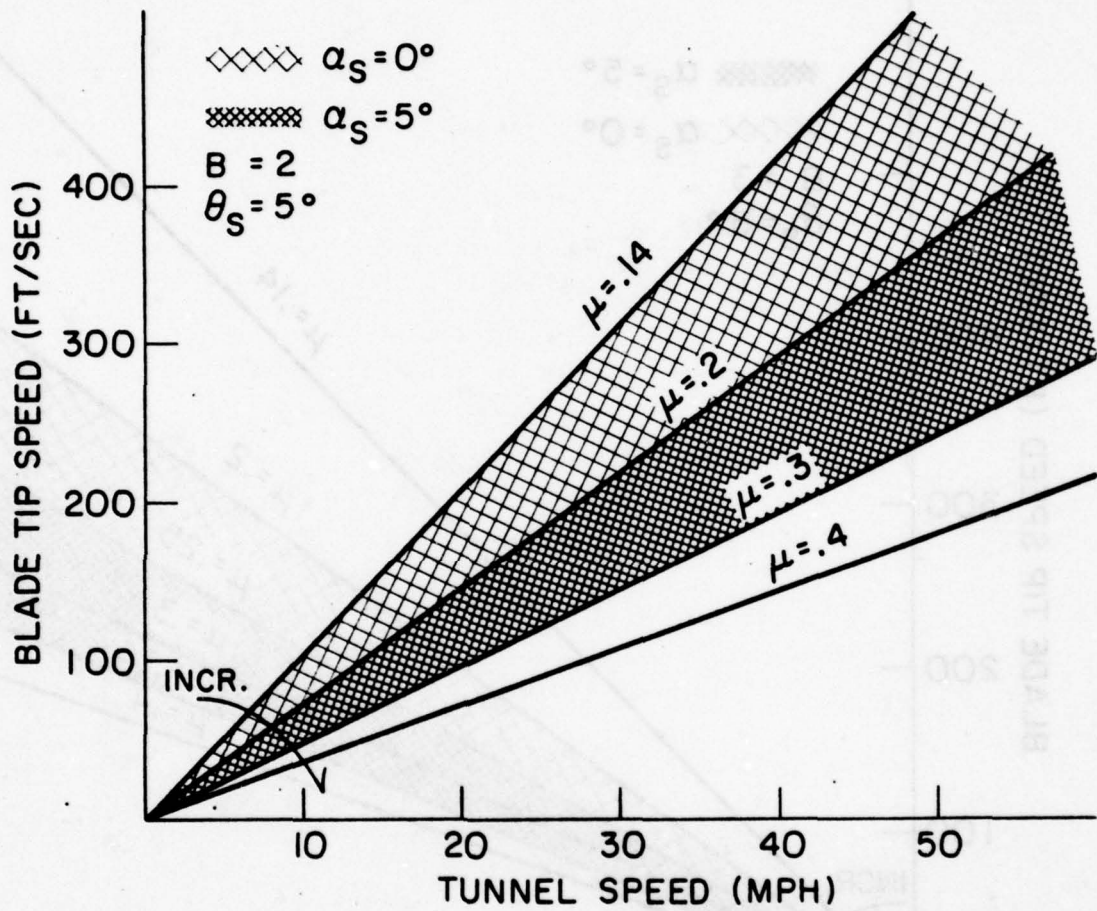


FIG. 4 BLADE SLAP BOUNDARY MAPPING

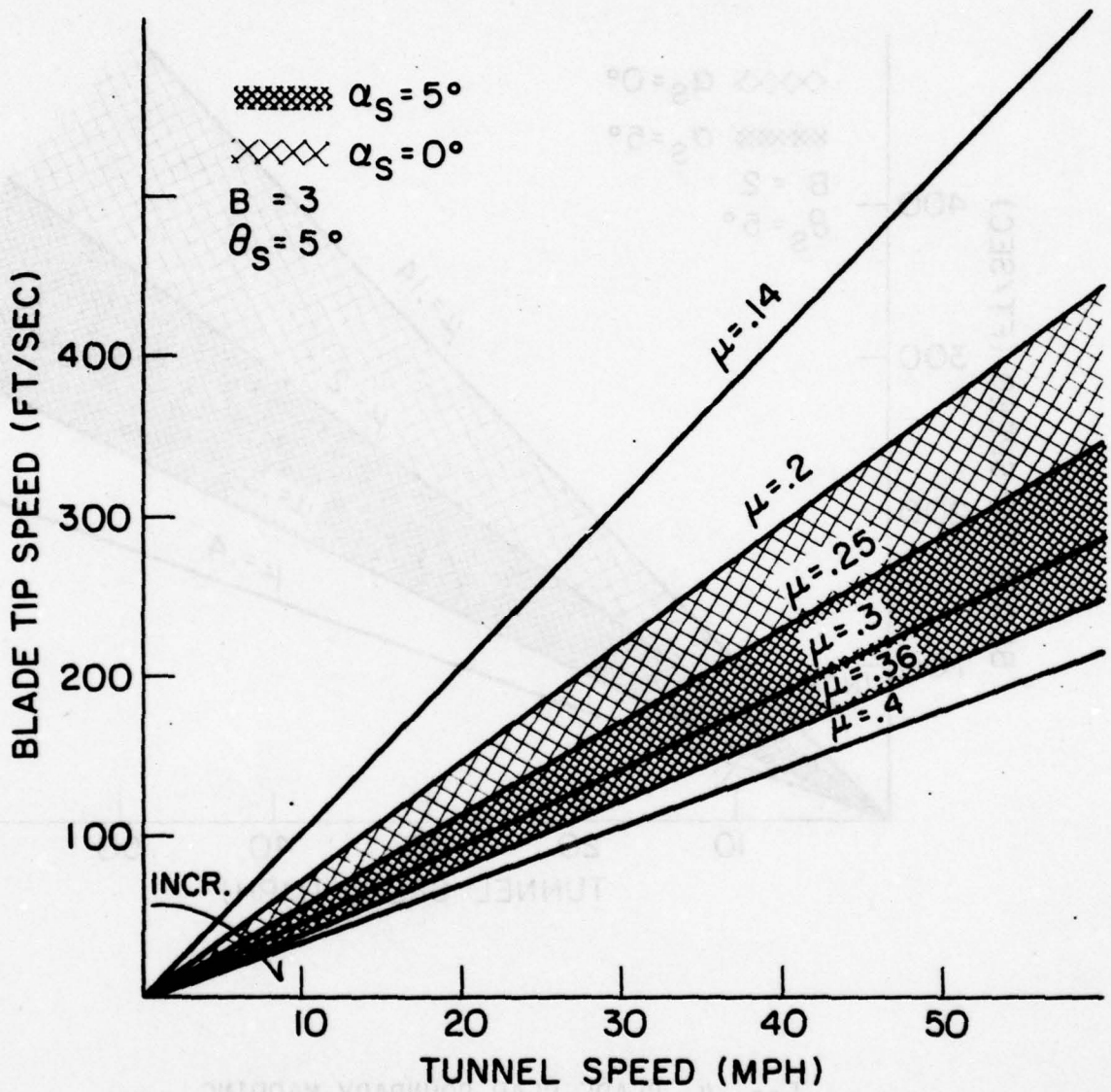


FIG. 5 BLADE SLAP BOUNDARY MAPPING

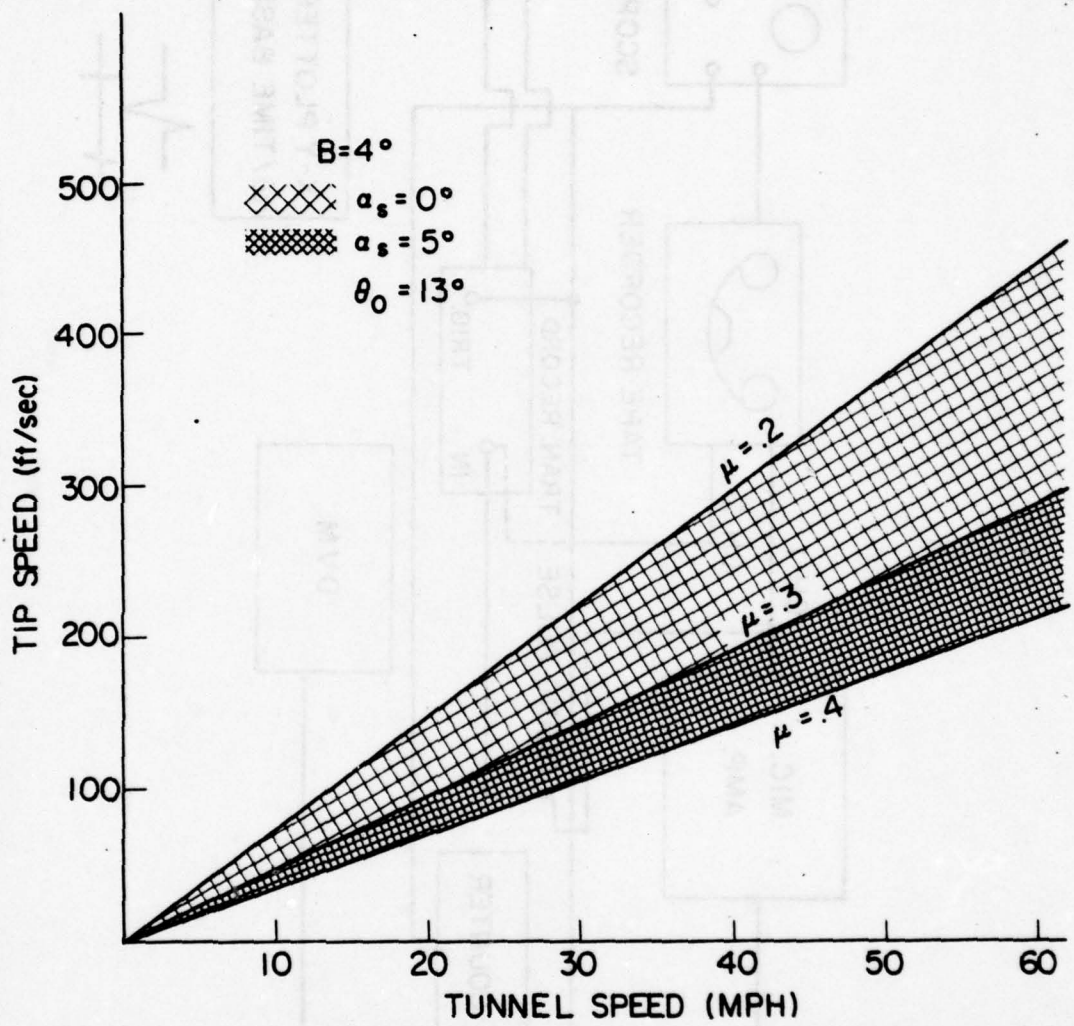


FIG. 6 BLADE SLAP BOUNDARY MAPPING

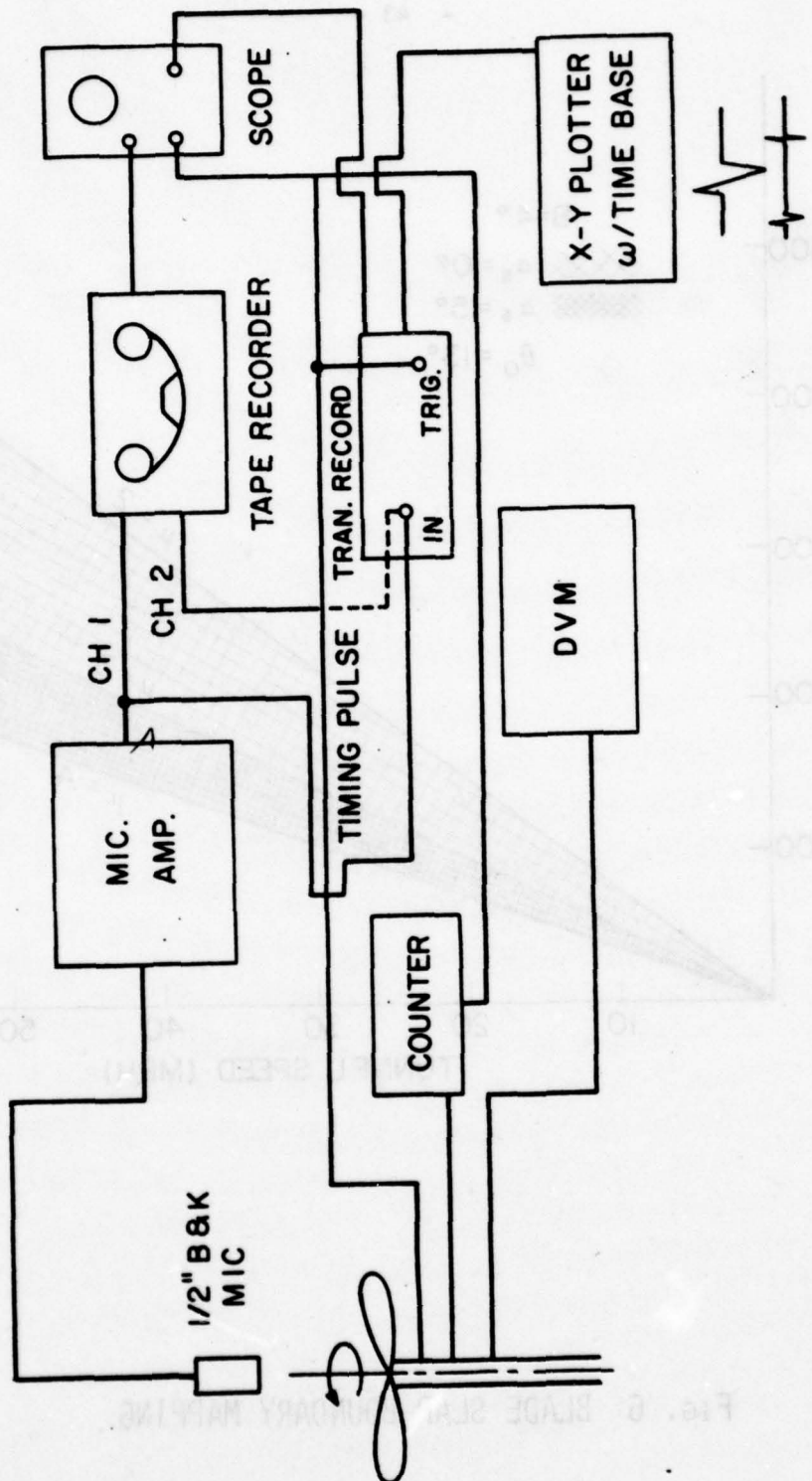


FIG. 7 SCHEMATIC OF INSTRUMENTATION USED IN DATA ACQUISITION

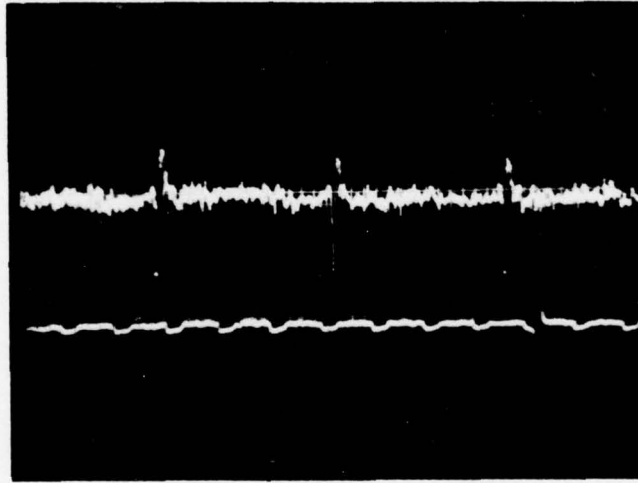


FIG. 8 TYPICAL PRESSURE-TIME HISTORY TRACE OF BLADE SLAP

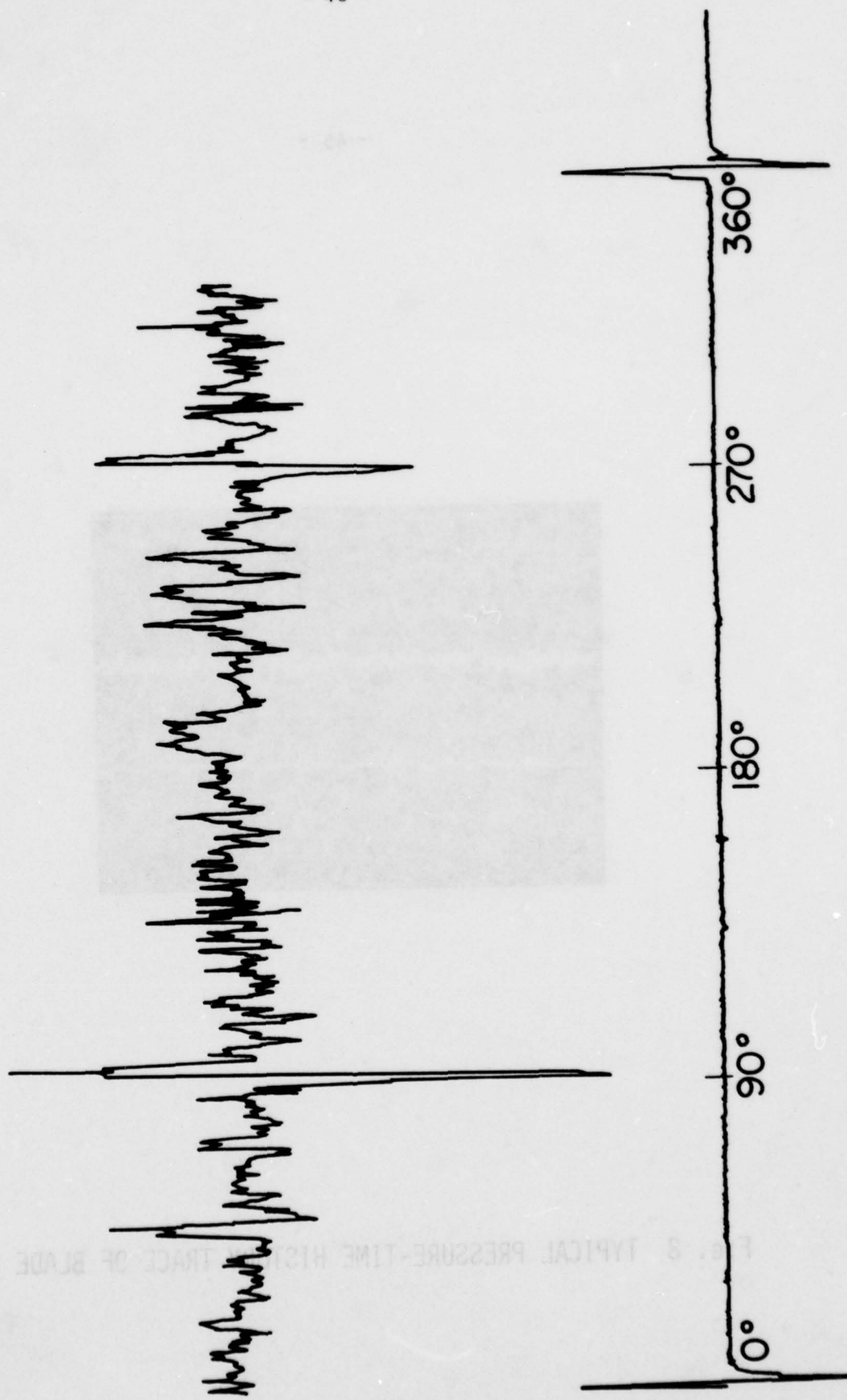


FIG. 9 TYPICAL TRANSIENT RECORDER TRACE OF BLADE SLAP PROFILE

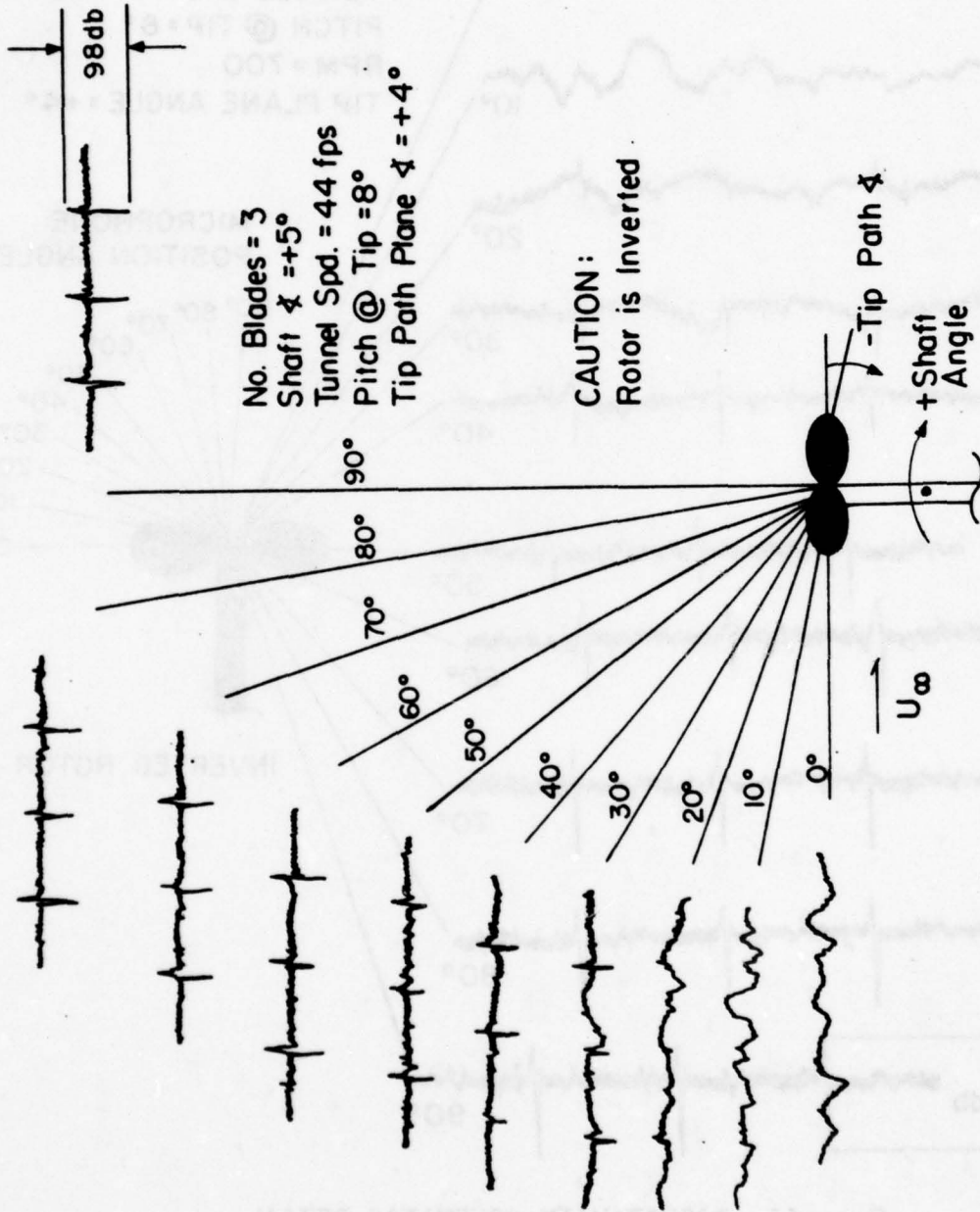


FIG. 10 MODEL ROTOR DIRECTIVITY SCHEMATIC

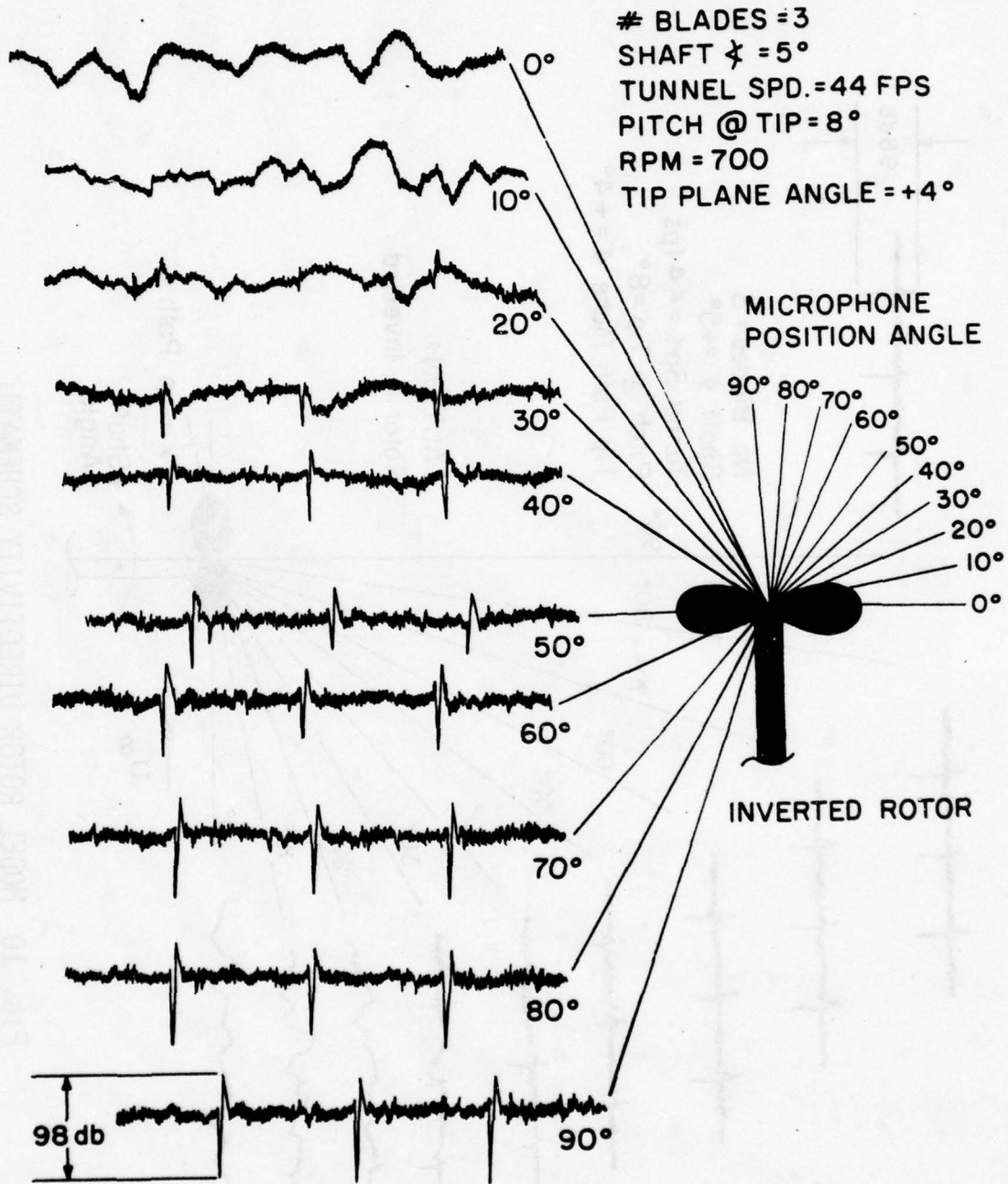
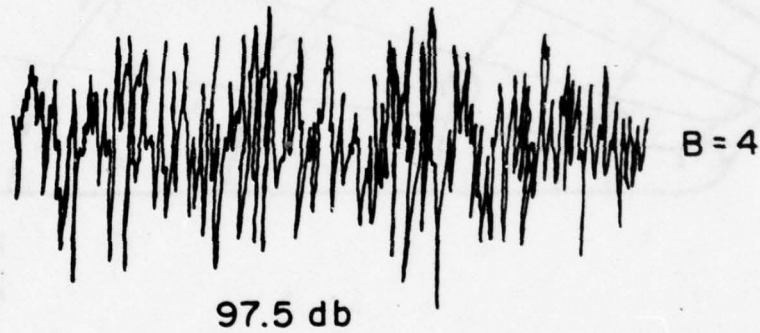
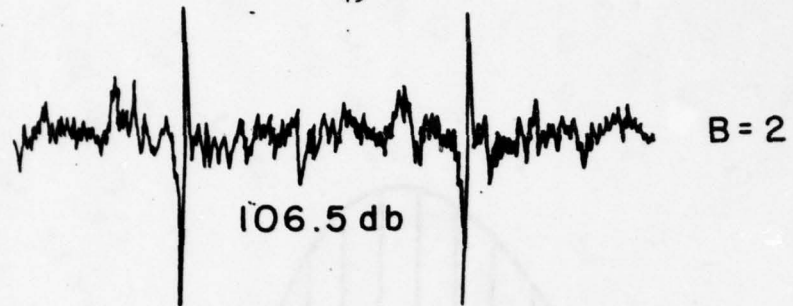


FIG. 11 DIRECTIVITY SCHEMATIC DETAIL



$\alpha_s = 0^\circ$
 $\theta_s = 5^\circ$
RPM = 1300
 $U_T = 51.3 \text{ fps}$

FIG. 12 PRESSURE-TIME HISTORY STUDY OF NUMBER OF BLADE EFFECT

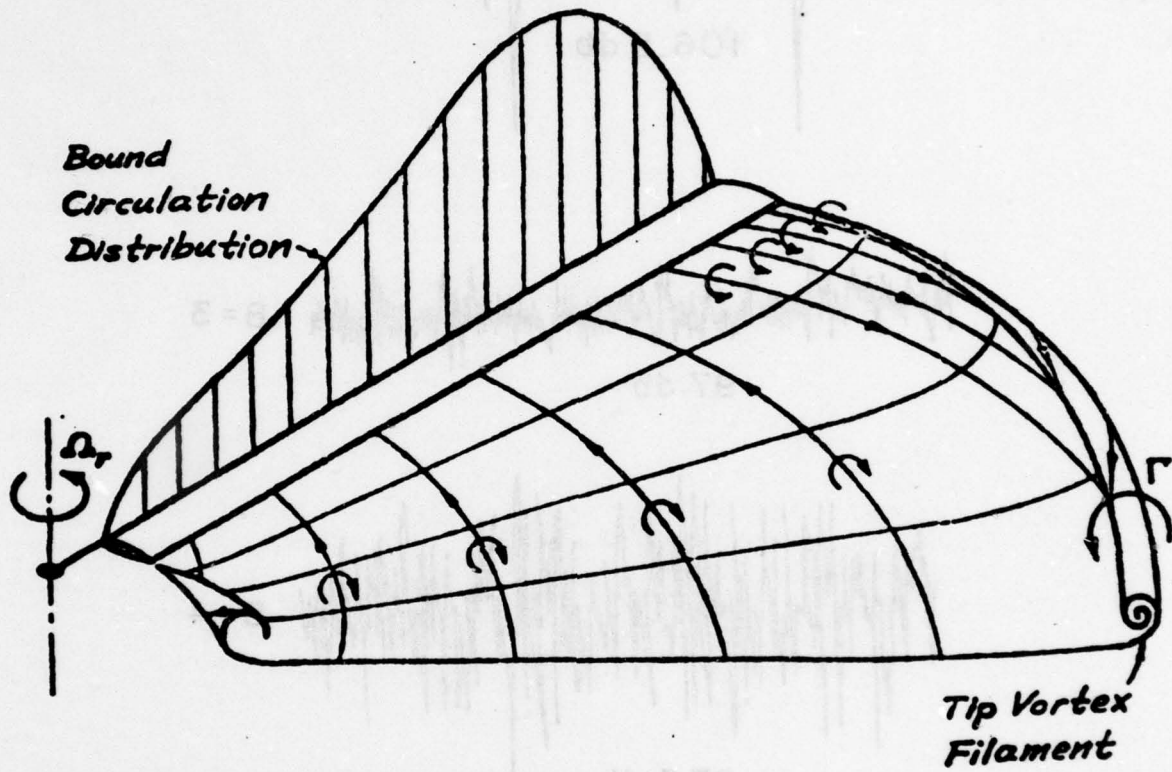


FIG. 13 ROLL-UP OF THE WAKE VORTEX SHEET AND THE FORMATION OF THE TIP VORTEX

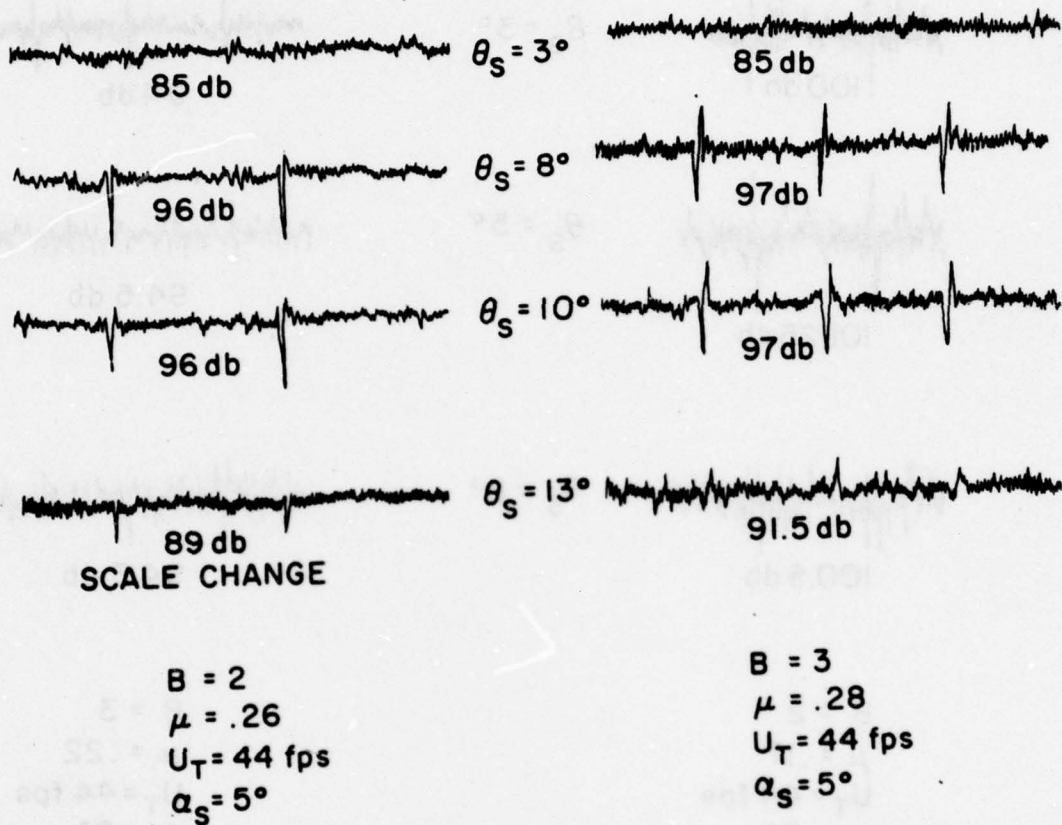
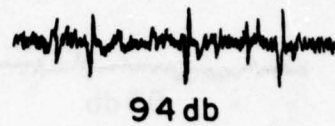


FIG. 14 PRESSURE-TIME HISTORY STUDY OF BLADE PITCH EFFECT
(5° SHAFT ANGLE)



$\theta_s = 3^\circ$



$\theta_s = 5^\circ$



$\theta_s = 8^\circ$



$B = 2$

$\mu = .17$

$U_T = 44 \text{ fps}$

$\alpha_s = 0^\circ$

$B = 3$

$\mu = .22$

$U_T = 44 \text{ fps}$

$\alpha_s = 0^\circ$

FIG. 15 PRESSURE-TIME HISTORY STUDY OF BLADE PITCH EFFECT
(0° SHAFT ANGLE)

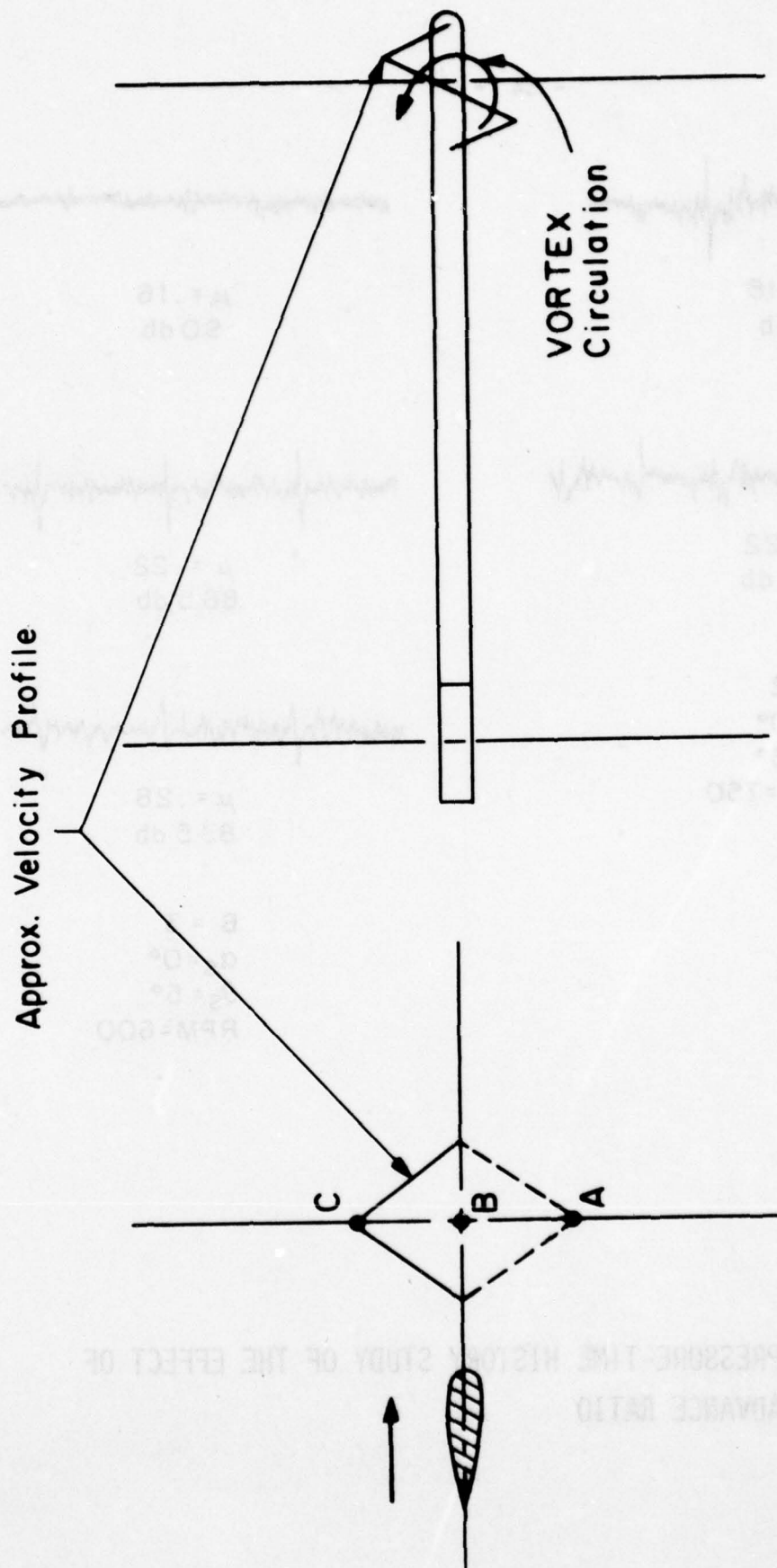
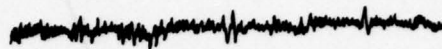


FIG. 16 VORTEX CORE AXIS PARALLEL TO DIRECTION OF BLADE MOTION



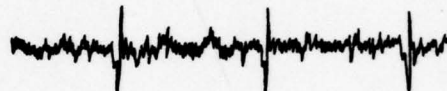
$\mu = .18$
90db



$\mu = .16$
90db

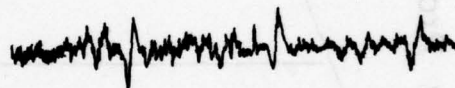


$\mu = .22$
85.5 db



$\mu = .22$
86.5 db

$B = 2$
 $\alpha_S = 0^\circ$
 $\theta_S = 5^\circ$
RPM = 750



$\mu = .28$
83.5 db

$B = 3$
 $\alpha_S = 0^\circ$
 $\theta_S = 5^\circ$
RPM = 600

FIG. 17 PRESSURE-TIME HISTORY STUDY OF THE EFFECT OF ADVANCE RATIO

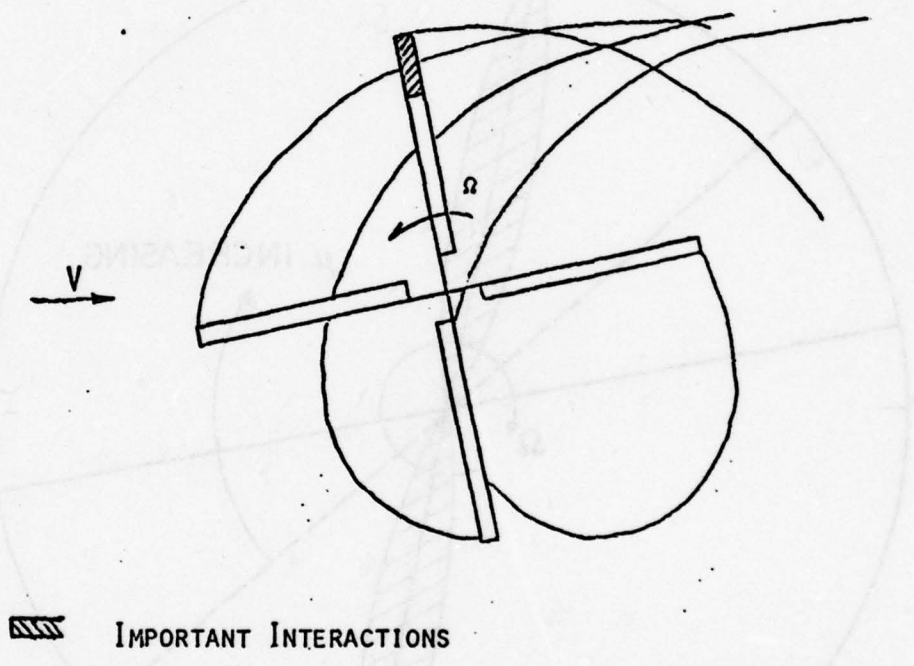


FIG. 18 SINGLE ROTOR BLADE/VORTEX INTERACTION
(RIGID WAKE ASSUMPTION)

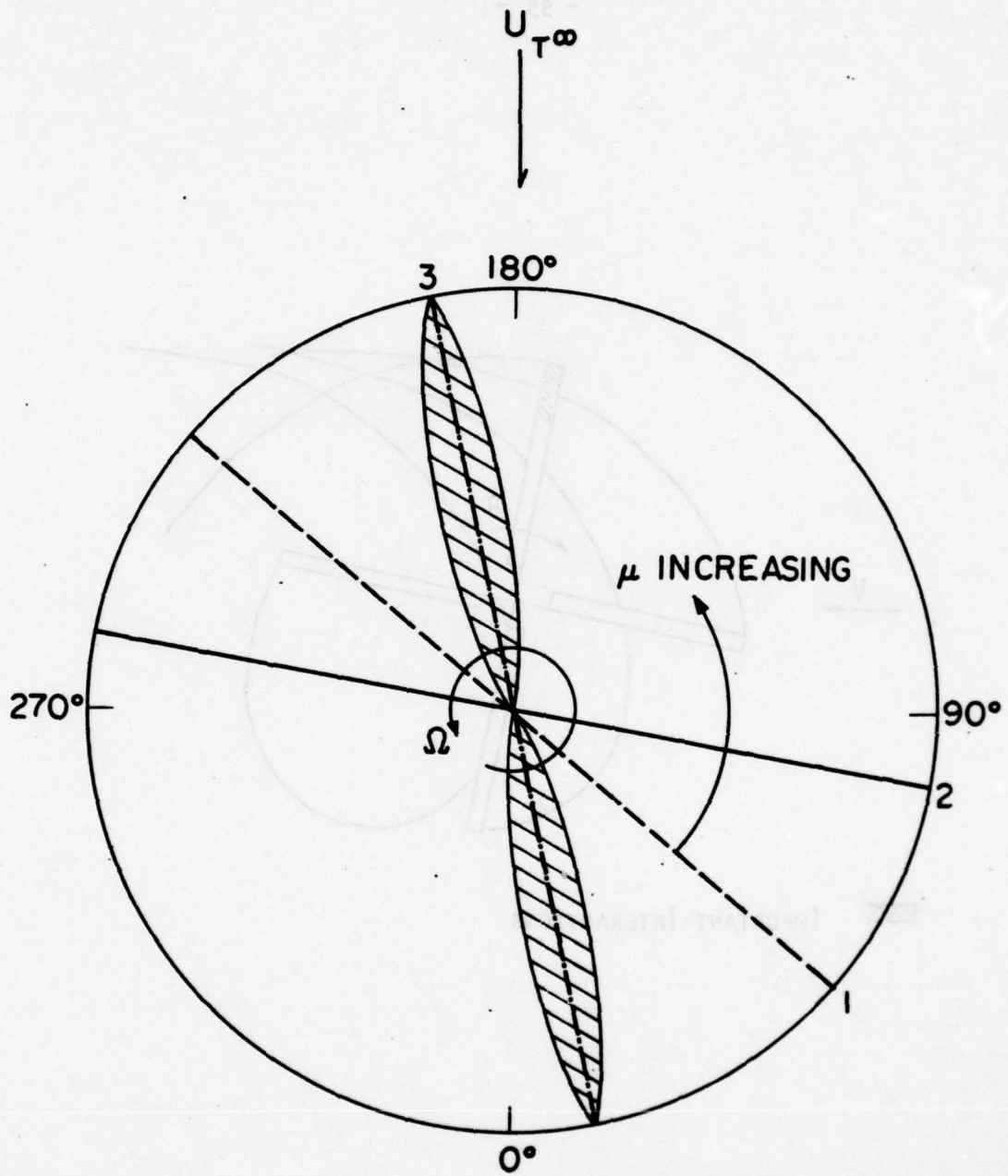


FIG. 19 BLADE/VORTEX AZIMUTHAL INTERACTION ANGLES

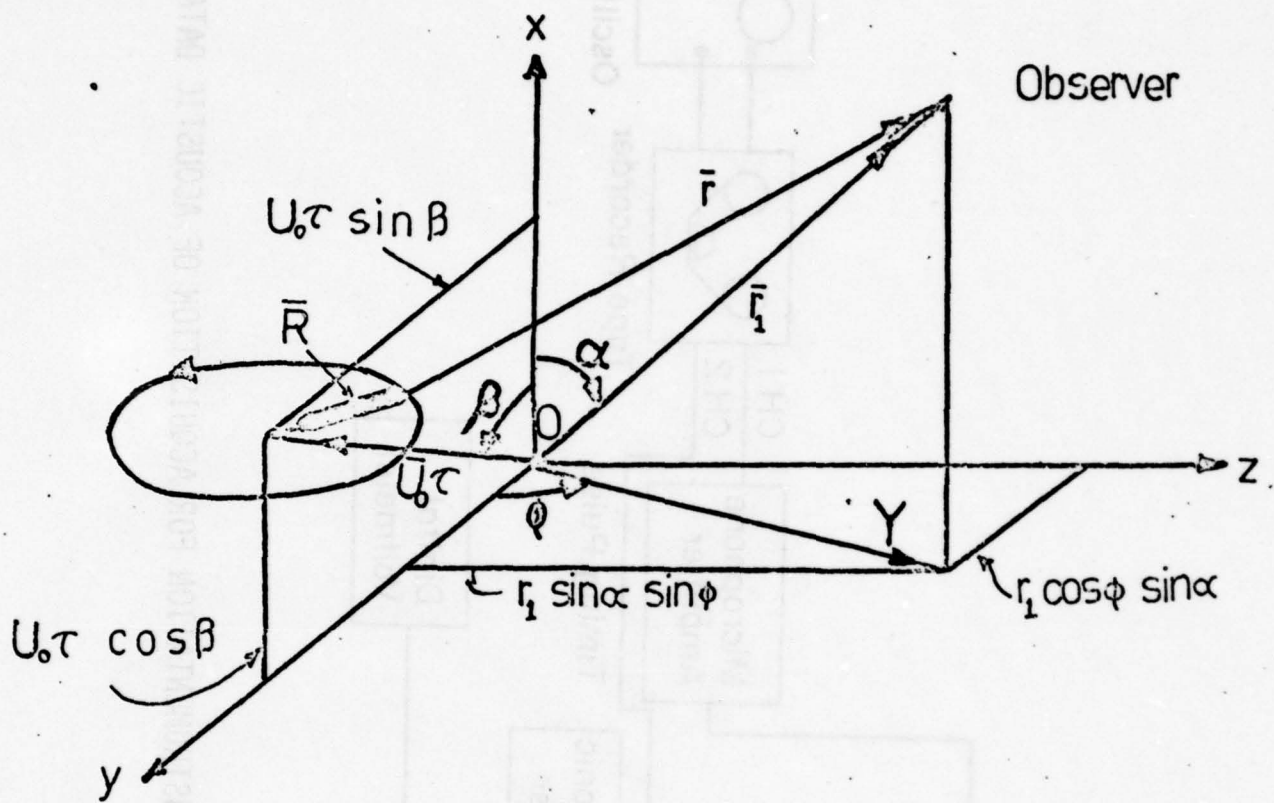


FIG. 20 COORDINATE SYSTEM FOR ROTATIONAL NOISE

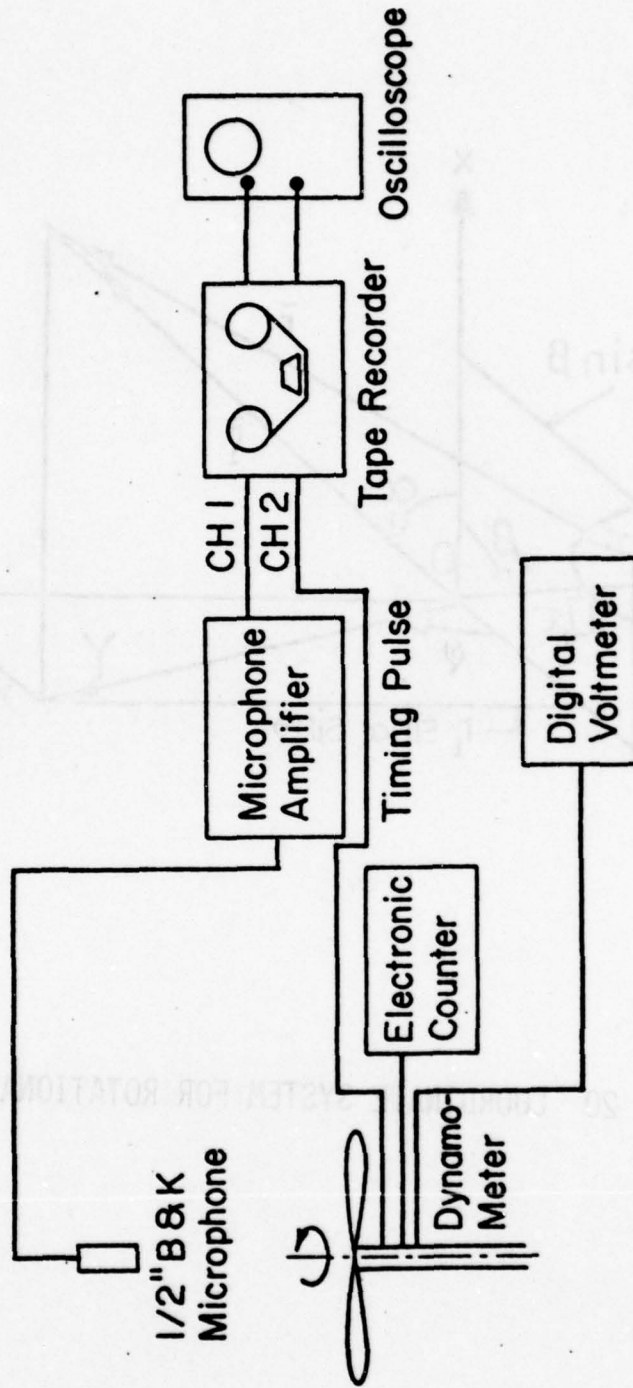


Fig. 21 SCHEMATIC OF INSTRUMENTATION FOR ACQUISITION OF ACOUSTIC DATA

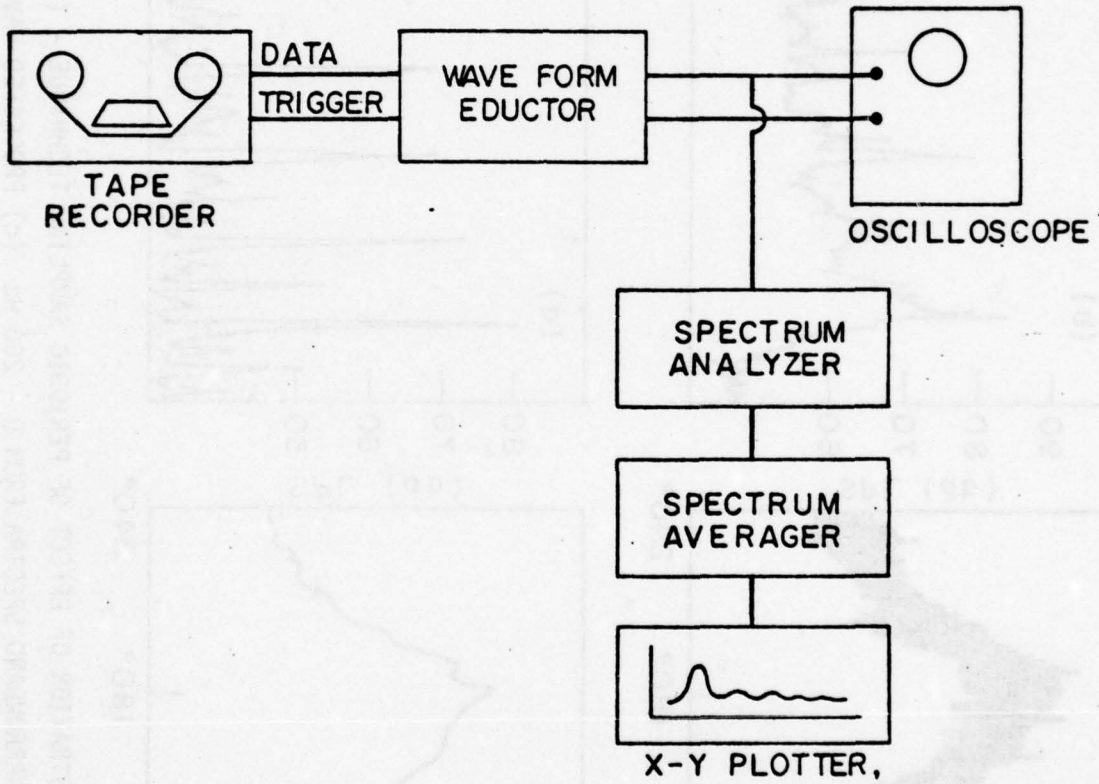


FIG. 22 SCHEMATIC OF INSTRUMENTATION FOR PROCESSING ROTATIONAL NOISE

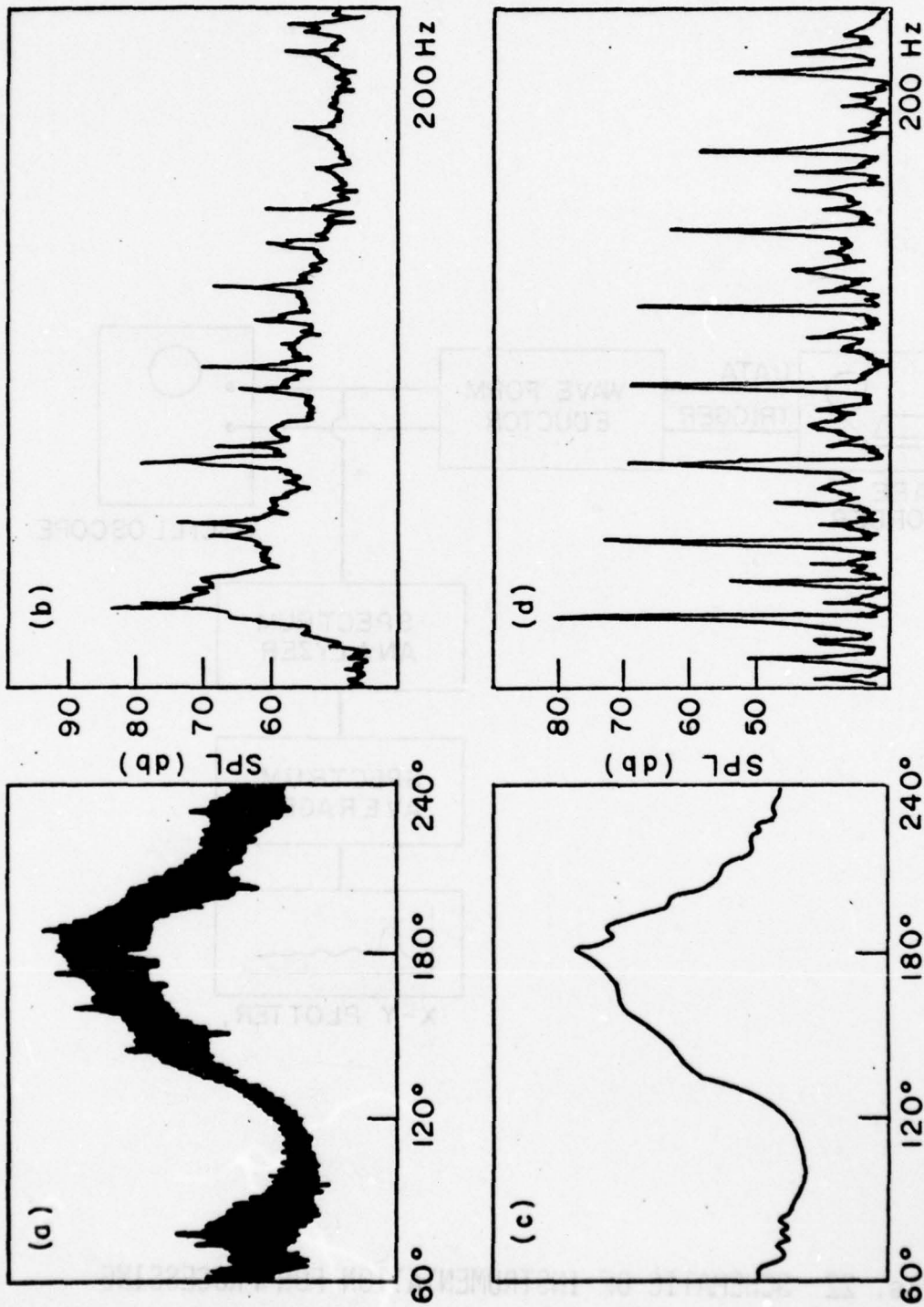


FIG. 23 - ILLUSTRATION OF EFFECT OF PERIODIC SAMPLING TECHNIQUE - (a) WAVEFORM OF RAW DATA
(b) CORRESPONDING NARROWBAND SPECTRA FROM 0 - 200 Hz (c) PROCESSED WAVEFORM and
(d) SUBSEQUENT NARROWBAND SPECTRA

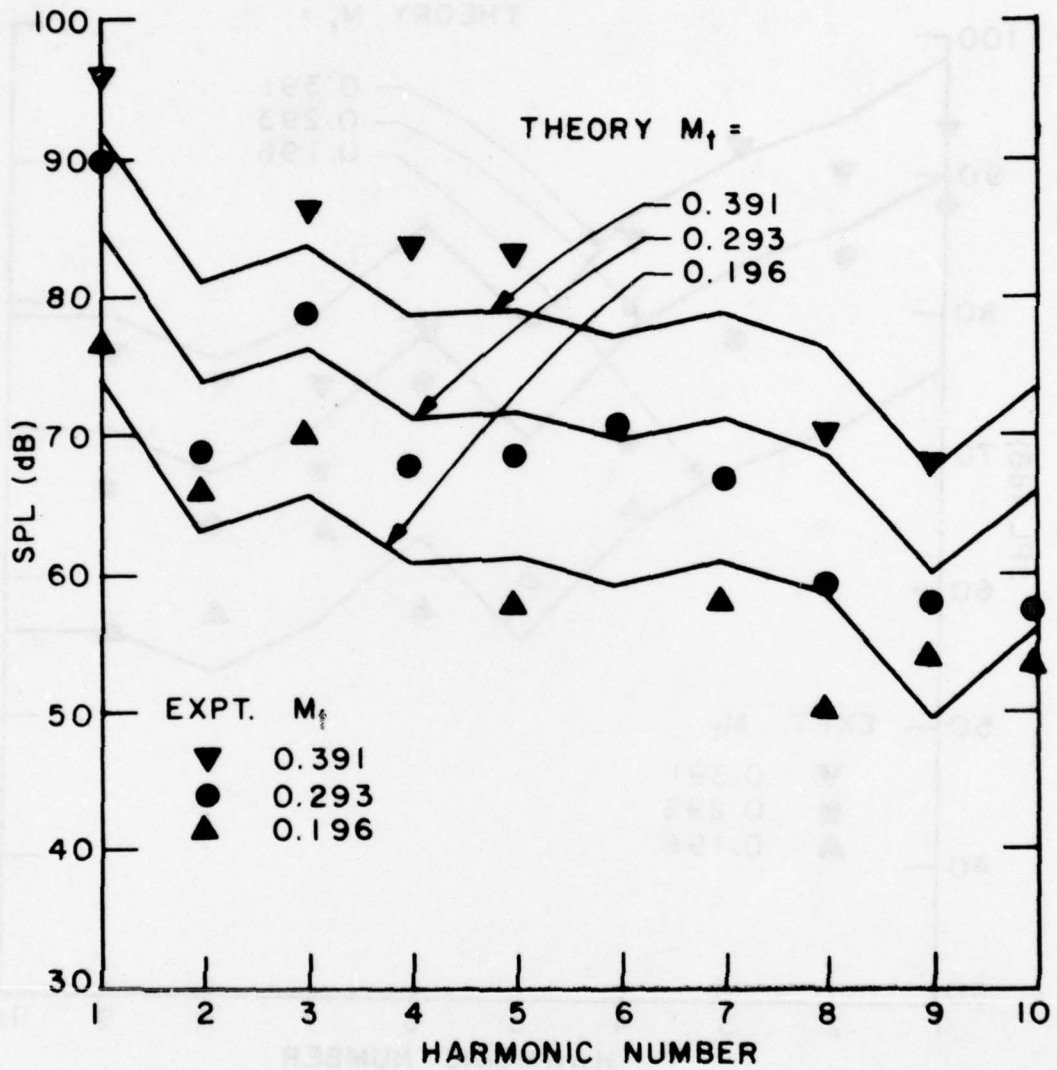


FIG. 24 MACH NUMBER SCALING FOR ROTATIONAL HARMONICS OF A TWO-BLADED ROTOR ON AXIS.

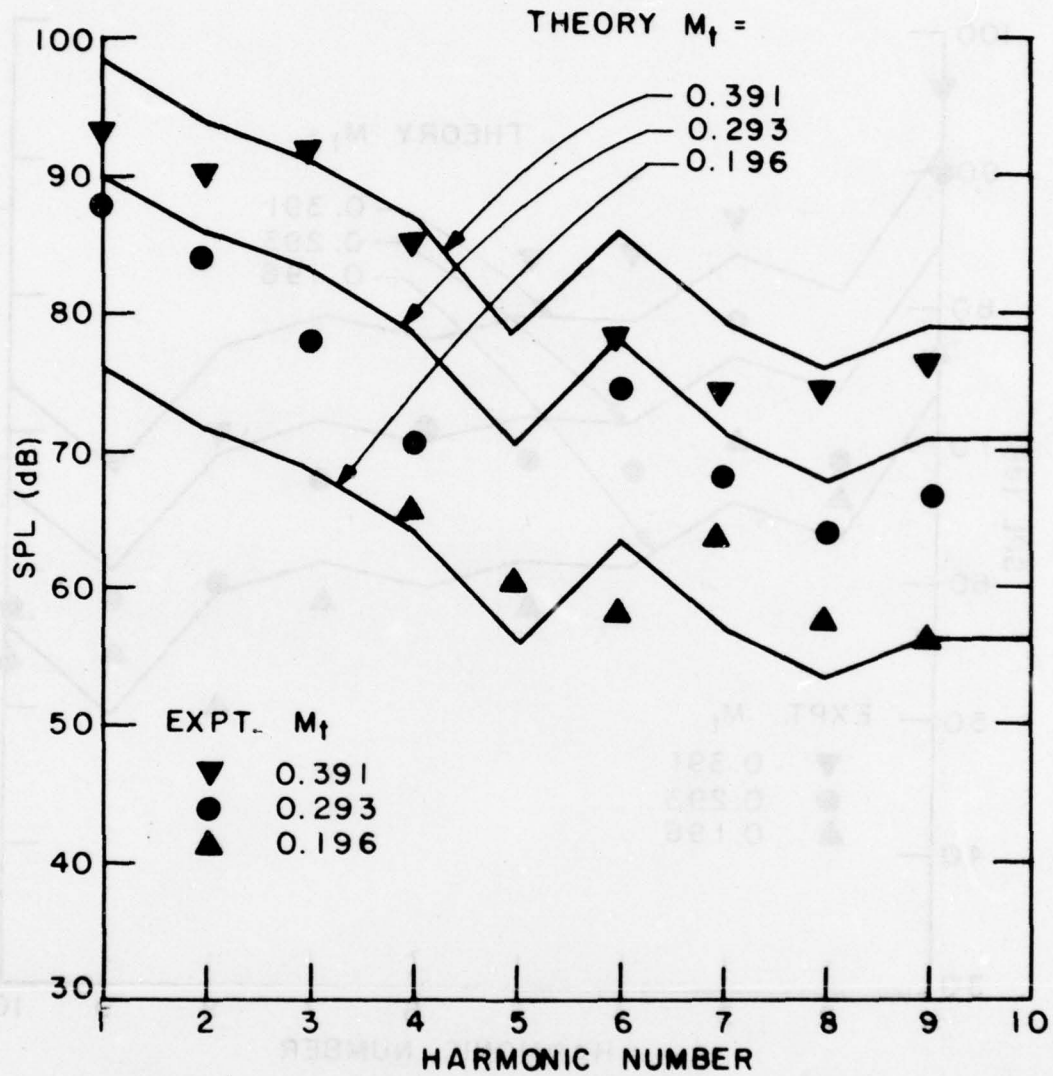


FIG. 25 MACH NUMBER SCALING FOR ROTATIONAL HARMONICS OF A TWO-BLADED ROTOR OFF AXIS.

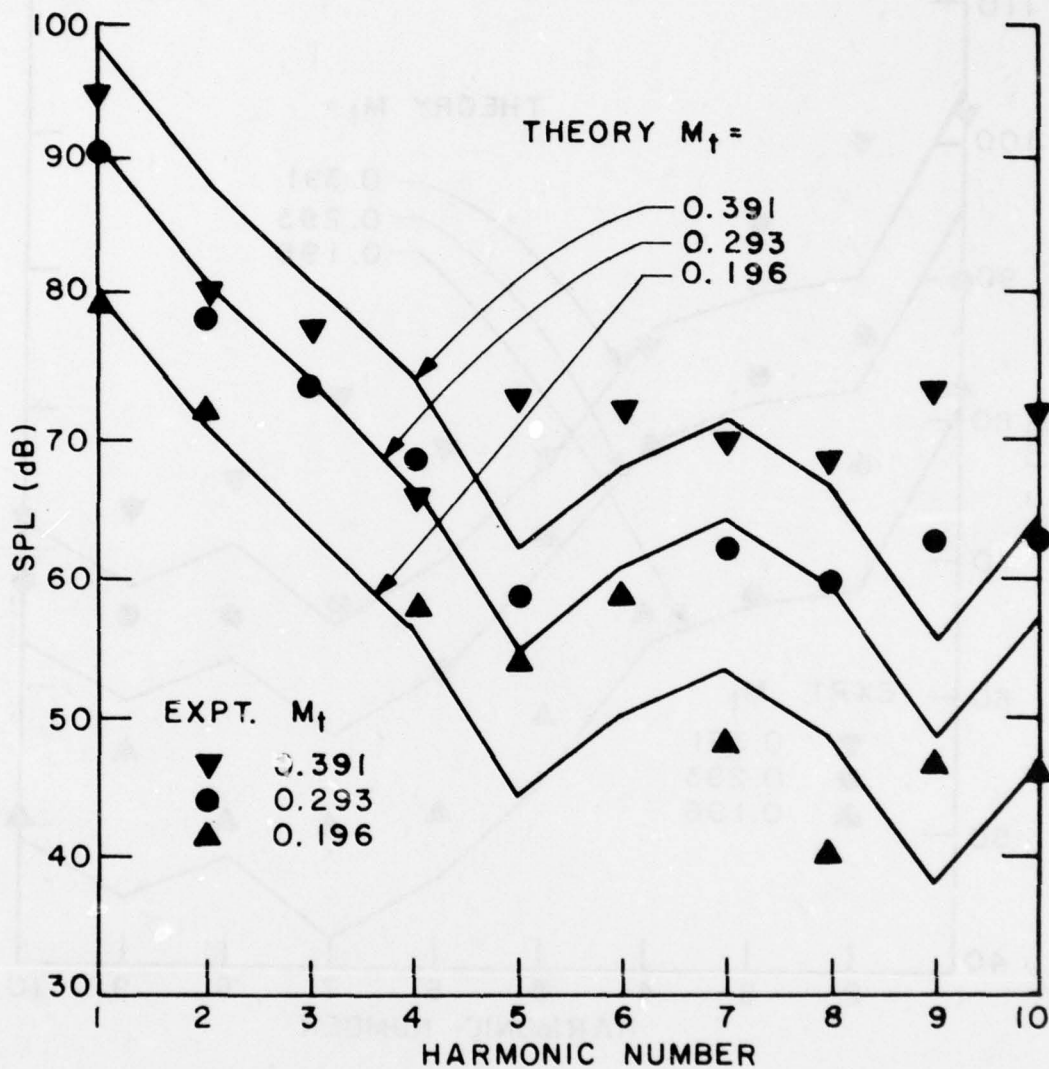


FIG. 26 MACH NUMBER SCALING FOR ROTATIONAL HARMONICS OF A THREE - BLADED ROTOR ON AXIS.

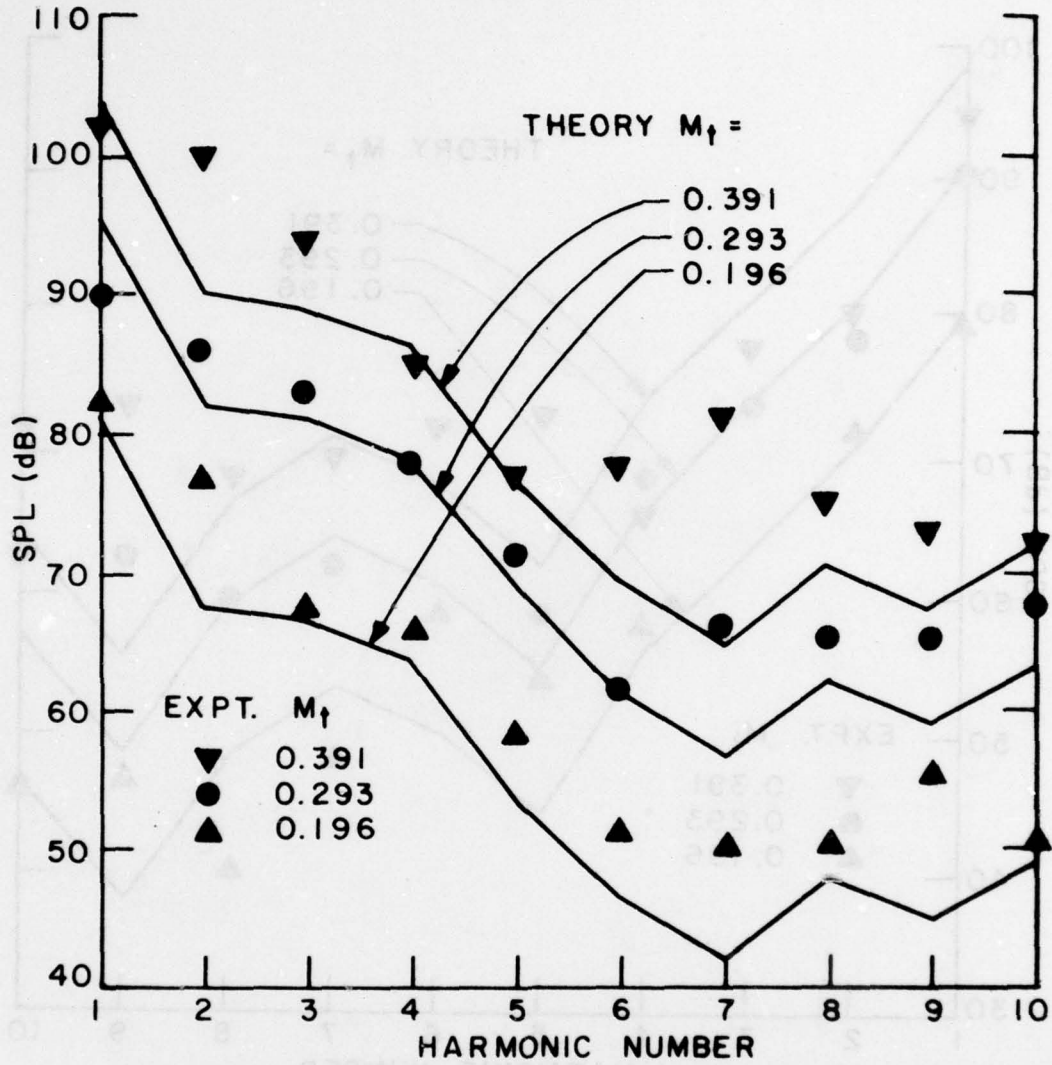


FIG. 27 MACH NUMBER SCALING FOR ROTATIONAL HARMONICS OF A THREE-BLADED ROTOR OFF AXIS.

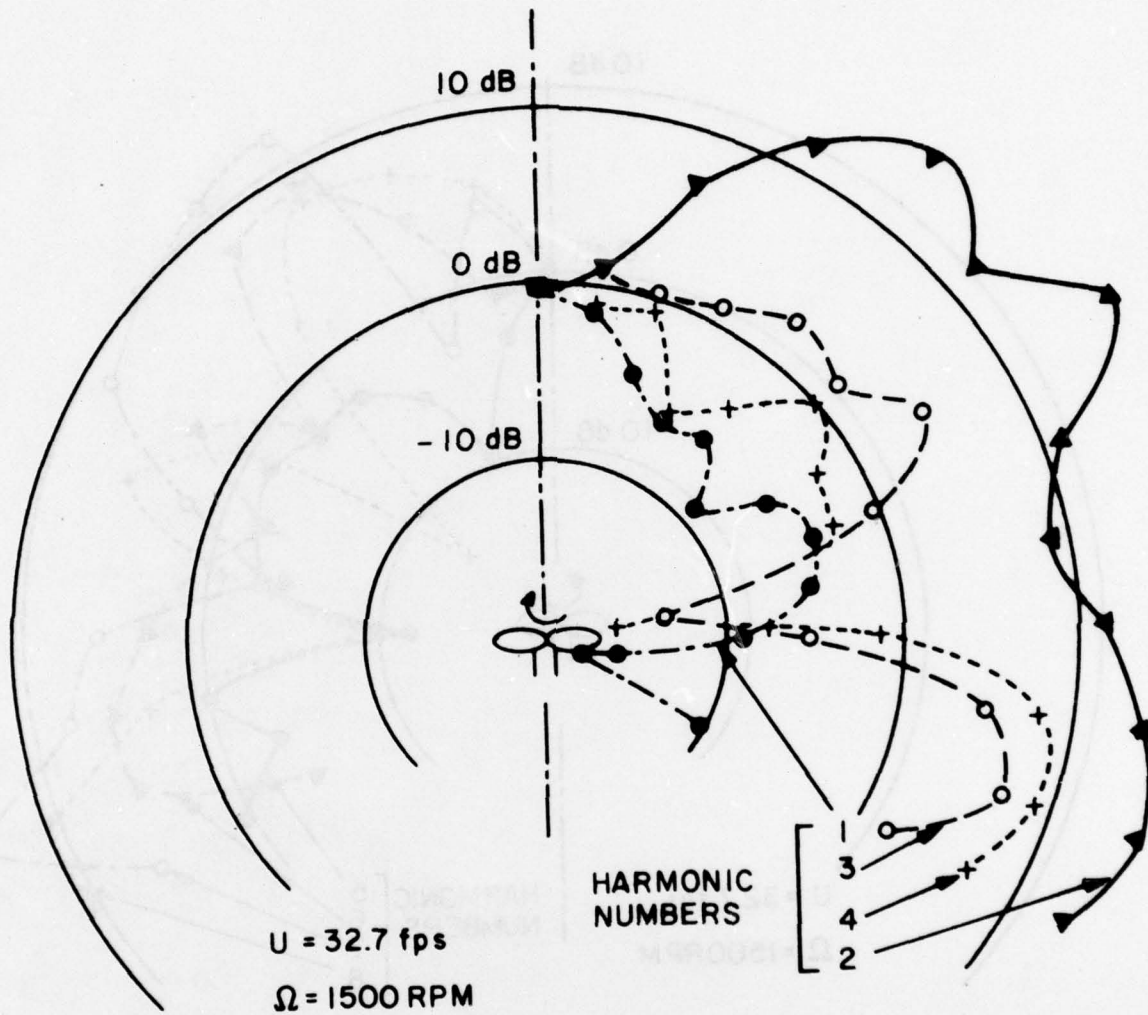


FIG. 28 DIRECTIVITY OF LOWER HARMONICS OF A TWO-BLADED ROTOR.

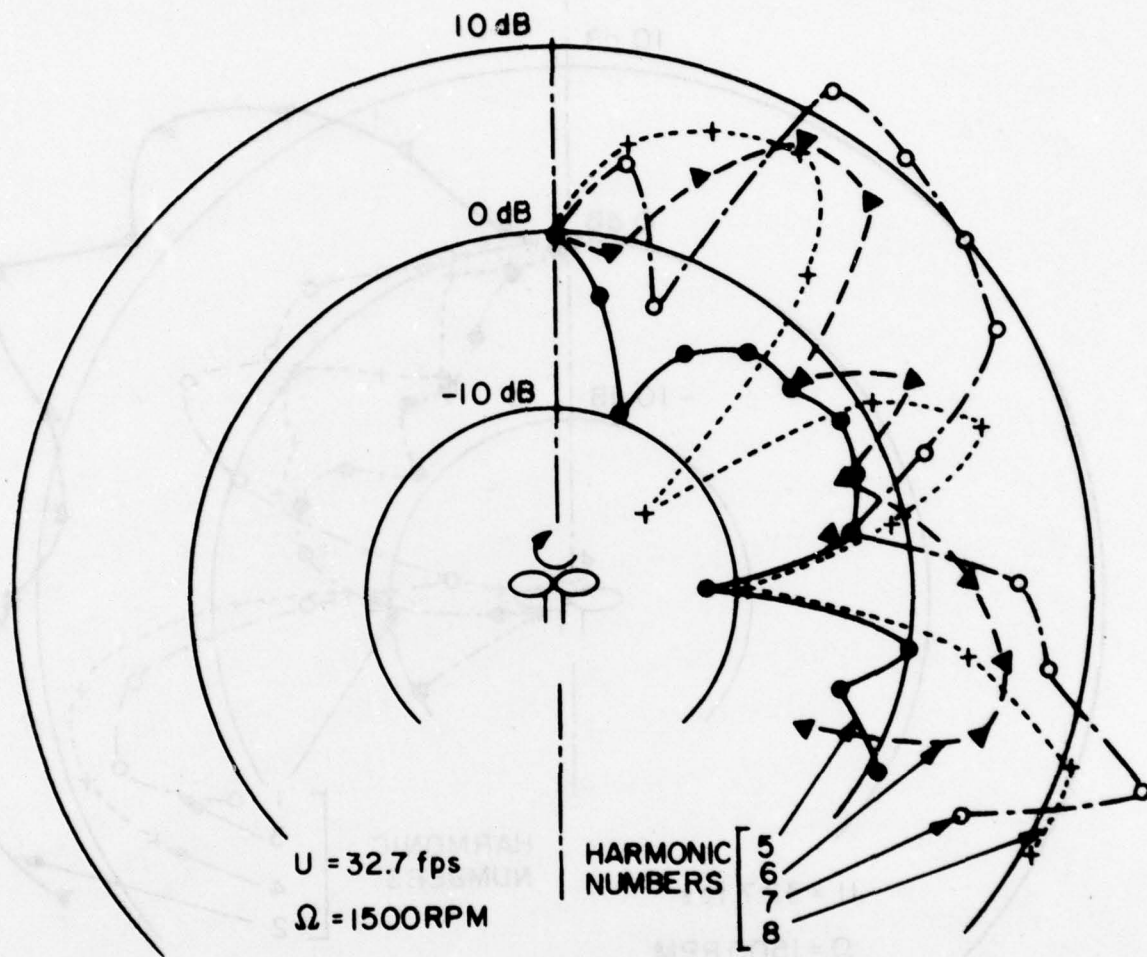


FIG. 29 DIRECTIVITY OF HIGHER HARMONICS OF A TWO-BLADED ROTOR.

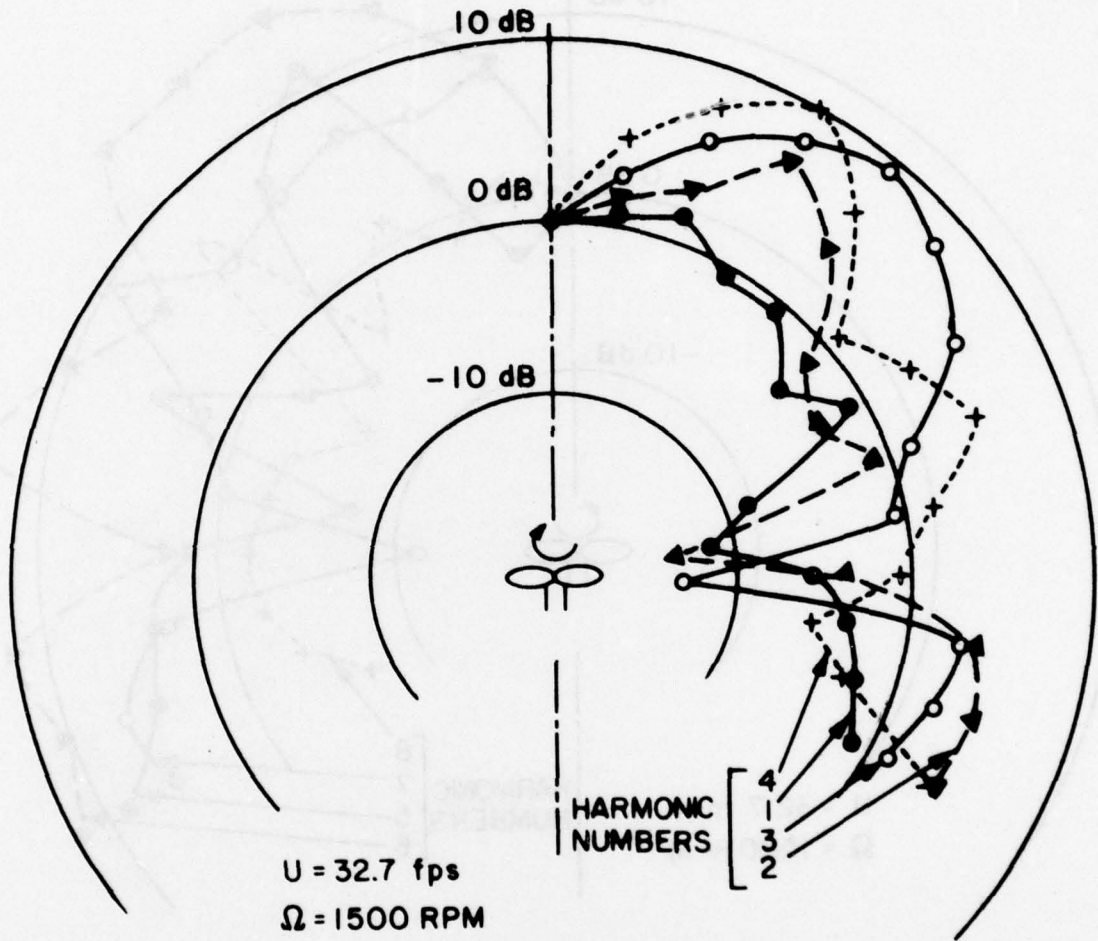


FIG. 30 DIRECTIVITY OF LOWER HARMONICS OF A THREE-BLADED ROTOR.

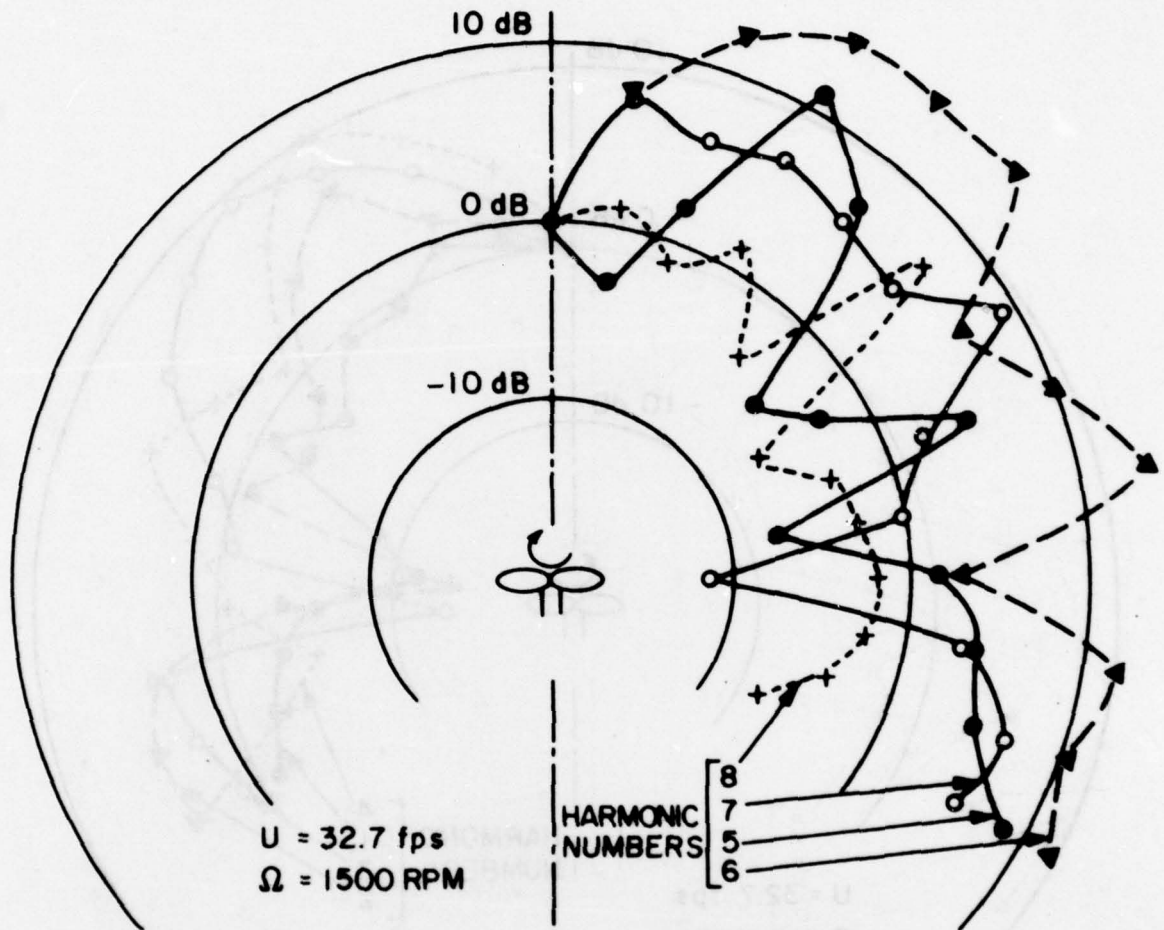


FIG. 31 DIRECTIVITY OF HIGHER HARMONICS OF A THREE-BLADED ROTOR.

APPENDIX A

An attempt was made to quantify the measurement of blade slap. Quantitative correlations were obtained using the data acquired in the directivity search illustrated in Figures 10 and 11. Initially a crest factor was defined as the ratio of the peak db value to the root mean square value. Because of the impulsive nature of the blade slap signature it was felt that this would provide good correlation. The results are illustrated in Table A. In moving the microphone from a position where no blade slap was encountered to one of maximum blade slap the total SPL changed by 7% while the crest factor changed 5%. This may seem encouraging, however, when values of crest factor are matched against the corresponding profiles in Figures 10 and 11. It can be seen that the resolution provided by this method is insufficient to reflect the sometimes dramatic change in the profiles.

A second correlation was obtained using a defined form factor given as the ratio of the root mean square db value to the average value. It is of interest to note that for a square wave both crest factor and the form factor have values of unity. The results of the form factor correlation are shown in Table A and as expected, due to the periodic nature of the blade slap signature, very little correlation between the profiles and this parameter is evident. Finally the ratio of the peak db value to average value was obtained and is also shown in Table A. This technique seems to show merit in the detection of the onset of blade slap as is evidenced in the large change in sound pressure level as the microphone position varies from 20° to 30° . However, the total resolution

obtainable is still insufficient to justify the use of this correlation as a quantitative method of defining blade slap. Due to the time constraints present during this research effort, further investigation along these lines was not possible and hence a subjective definition of blade slap was used to perform the parametric studies herein.

TABLE A

CORRELATION FACTORS

<u>Microphone Position Angle (°)</u>	<u>Peak Sound Pressure Level (db)</u>	<u>Crest Factor</u>	<u>Form Factor</u>	<u>Peak/Avg.</u>
0	91.5	1.11	1.03	1.13
10	93.5	1.10	1.03	1.12
20	92	1.10	1.03	1.13
30	91	1.14	1.03	1.18
40	93	1.16	1.04	1.17
50	93.5	1.13	1.06	1.21
60	95.5	1.15	1.05	1.21
70	96	1.14	1.06	1.22
80	96.5	1.15	1.06	1.21
90	98	1.16	1.06	1.22

APPENDIX B

Lowson and Ollerhead [14] give the theoretical result for the sound pressure level of the m^{th} harmonic due to the steady and fluctuation forces as

$$\begin{aligned}
 c_m = & \sum_{\lambda=0}^{\infty} \frac{i^{[mB-\lambda]}}{4\pi} \left\{ \frac{mB\Omega x}{a_o r^2} \left\{ i a_{\lambda T} \left(J_{mB-\lambda} + [-1]^{\lambda} J_{mB+\lambda} \right) - b_{\lambda T} \left(J_{mB-\lambda} - [-1]^{\lambda} J_{mB+\lambda} \right) \right\} \right. \\
 & - \left. \left\{ \frac{i a_{\lambda D}}{Rr} \left((mB-\lambda) J_{mB-\lambda} + [-1]^{\lambda} (mB+\lambda) J_{mB+\lambda} \right) \right. \right. \\
 & - \left. \frac{b_{\lambda D}}{Rr} \left((mB-\lambda) J_{mB-\lambda} - [-1]^{\lambda} (mB+\lambda) J_{mB+\lambda} \right) \right\} + \frac{mB\Omega y}{a_o r^2} \left\{ a_{\lambda C} \left(J_{mB-\lambda} + [-1]^{\lambda} J_{mB+\lambda} \right) \right. \\
 & \left. \left. + i b_{\lambda C} \left(J_{mB-\lambda} - [-1]^{\lambda} J_{mB+\lambda} \right) \right\} \right\} \tag{B1}
 \end{aligned}$$

where the argument of the Bessel functions is $mB \frac{M}{y/r}$. The force components are defined as

$$\begin{aligned}
 \text{Thrust} \quad T[\psi] &= a_{oT} + \sum_{\lambda=1}^{\infty} a_{\lambda T} \cos \lambda \psi + b_{\lambda T} \sin \lambda \psi \\
 \text{Drag} \quad D[\psi] &= a_{oD} + \sum_{\lambda=1}^{\infty} a_{\lambda D} \cos \lambda \psi + b_{\lambda D} \sin \lambda \psi \\
 \text{Radial Components} \quad C[\psi] &= a_{oC} + \sum_{\lambda=1}^{\infty} a_{\lambda C} \cos \lambda \psi + b_{\lambda C} \sin \lambda \psi
 \end{aligned}$$

The detailed directionality depends only on the Bessel functions which are themselves independent of the loading harmonics. Only the amplitude terms are affected by the loading. Because blade slap due to blade/vortex interaction results via a changing airloading harmonic distribution, the directionality associated with it does not vary significantly from that in the non blade slap case.

APPENDIX C

The prediction method given here is that of Pegg [16] based on the work of Wright [17]. The sound pressure level for each harmonic is

$$\begin{aligned} \text{SPL}_{\text{mB}} = & 20 \log \frac{\cos \theta}{ra_0} + 20 \log \text{mB} + 20 \log \text{NG} \\ & + 20 \log X_s \frac{\Delta L}{L_0} \frac{\Delta \psi}{\psi_0} - 20 \log P_0 \end{aligned} \quad (\text{C-1})$$

where the term $20 \log (X_s \frac{\Delta L}{L_0} \frac{\Delta \psi}{\psi_0})$ is the loading function. The spectrum function, X_s , is defined to be

$$X_s = \frac{\sin \pi(\text{mB} \frac{\Delta \psi}{\psi_0} - 1)}{4(\text{mB} \frac{\Delta \psi}{\psi_0} - 1)} - \frac{\sin \pi(\text{mB} \frac{\Delta \psi}{\psi_0} + 1)}{4(\text{mB} \frac{\Delta \psi}{\psi_0} + 1)} \quad (\text{C-2})$$

Figure B.1 is a schematic of the assumed loading resulting from blade/vortex interaction over azimuth angle $\Delta \psi$.